Observed HF radiation from an earthquake fault: properties; relation to fault structure; possible generation mechanisms

A.A. Gusev

Institute of Volcanology and Seismology, Russian Ac.Sci. and

Kamchatka Branch, Geophysical Service, Russian Ac.Sci.

Petropavlovsk-Kamchatsky, Russia

Defining HF

~~(1): $f > 0.3$Hz~~ **NO**

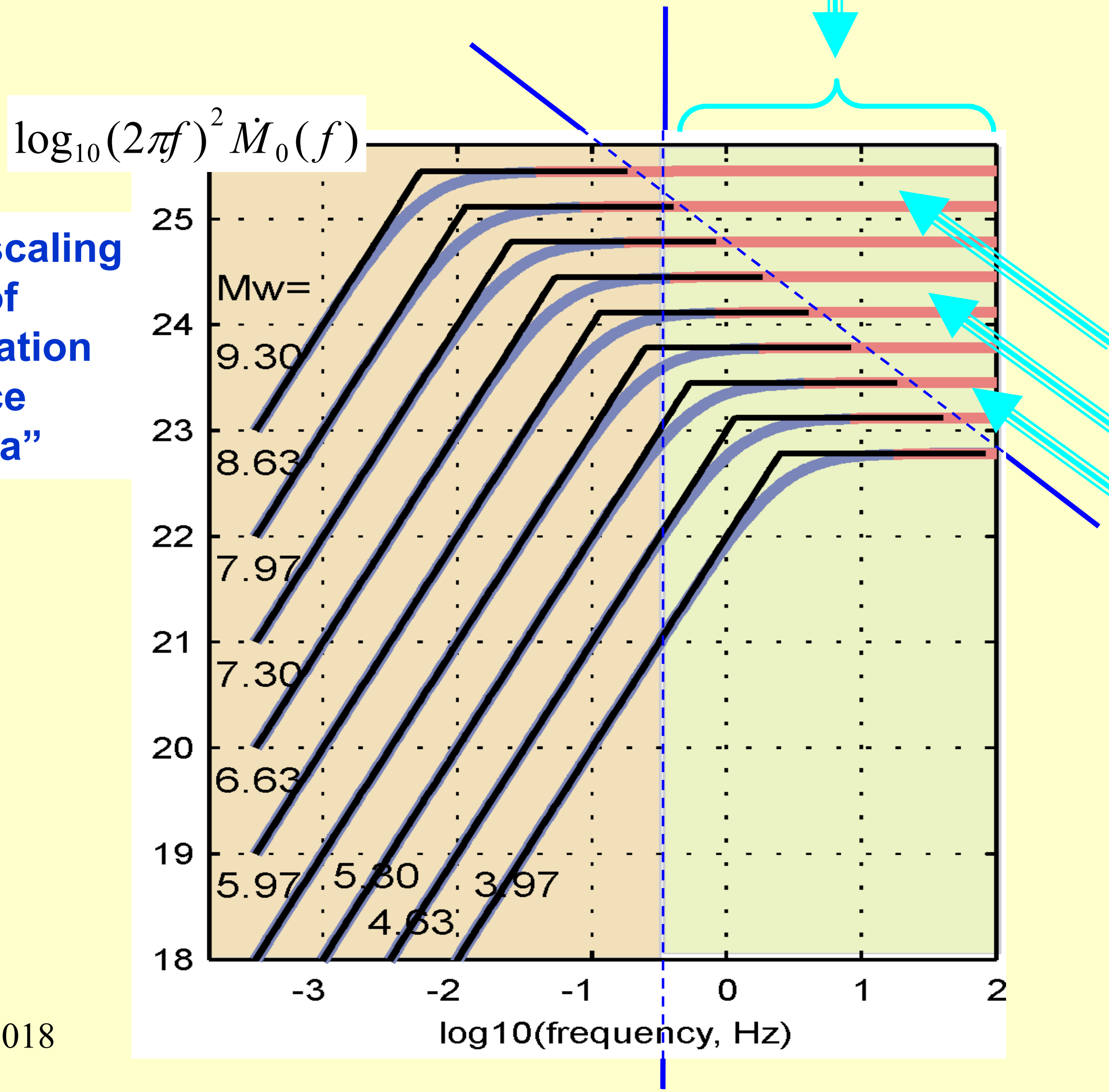

Idealized scaling law of "Acceleration source spectra"

(2): $f > (5\text{-}10) f_{corner}$ **YES**

Part A
Properties of HF radiation and their possible meaning

HF radiation: significant properties

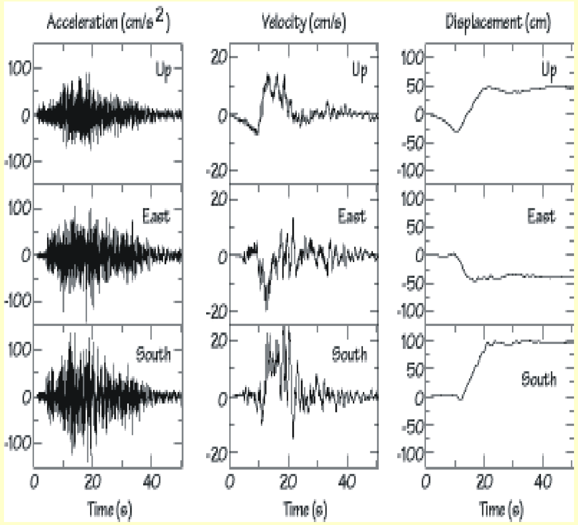

Anderson 1986

HF signal-accelerogram

- **1. Random appearance**
- **2. Distribution for amplitudes: non-Gaussian, moderately heavy-tailed**
- **3. Deteriorated or absent directivity**
- **4. Upper source-controlled spectral bound f_{max} ;** **(not to be confused with path-attenuation-controlled *fmax* feature)**
- **5. Lack of good correlation between local HF radiation capability and local slip rate over a fault**
- **6. Self-similar (fractal) time histories of HF power**

1. Random appearance of HF records

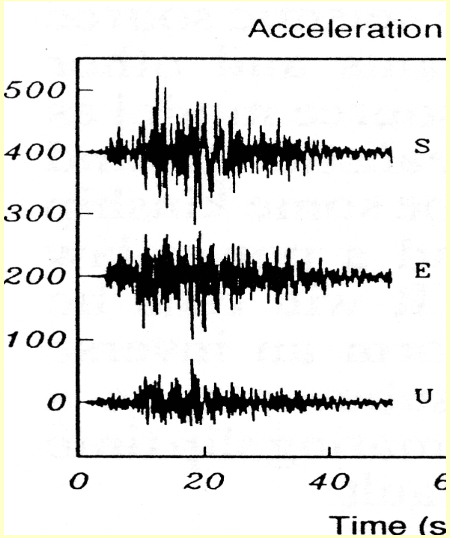

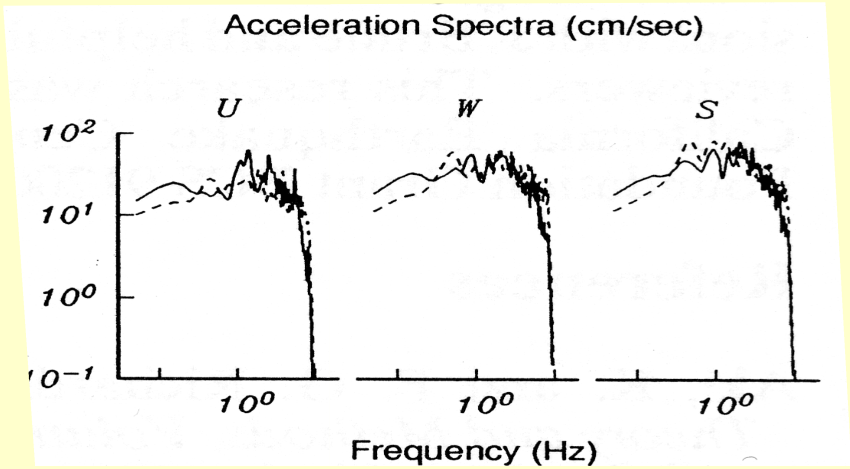

M8, 1985 Michocan, Mexico; Caleta de Campos, (Zeng&Anderson 1994)

HF records (accelerograms, HF-band-filtered teleseismic P-waves) look like **segments of modulated random noise**.

Accelerogram **spectra are broad-band**.

Accelerogram **spectra are slow-changing**; no **significant spectral peaks** are observed.

When effects of propagation can be ignored or compensated, these facts suggests:

random fault rupturing history,

with **multiplicity of scales** over space and time

2. Non-Gaussian distribution for amplitudes

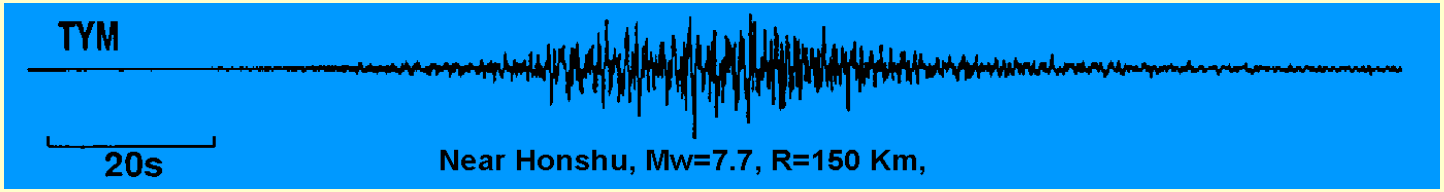

approximately Gaussian,

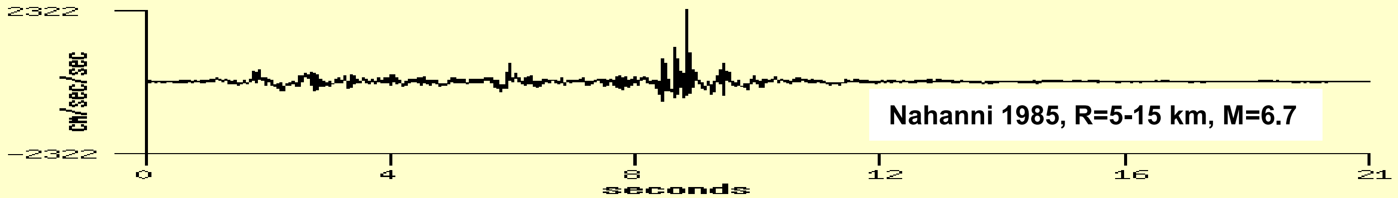

expressedly heavy-tailed non-Gaussian

Not infrequently, near-fault HF records show "spiky" behavior

[As propagation effects systematically "normalize" an accelerogram, only near-fault records on rock ground can be used to analyze statistics of the radiated HF signal]

When analyzed in more detail, distribution tails are only **moderately heavy**; assuming the power law upper tail:

$\mathrm{pdf}(x) \propto x^{-\alpha}$

the brackets for the α parameter are roughly 2.5-4.5.

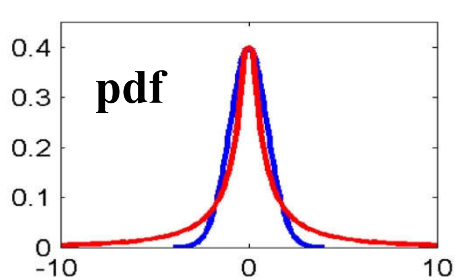

----------- Gaussian,
----------- Non-Gaussian, heavy-tailed

"Spiky" near-fault accelerograms : examples and possible causes

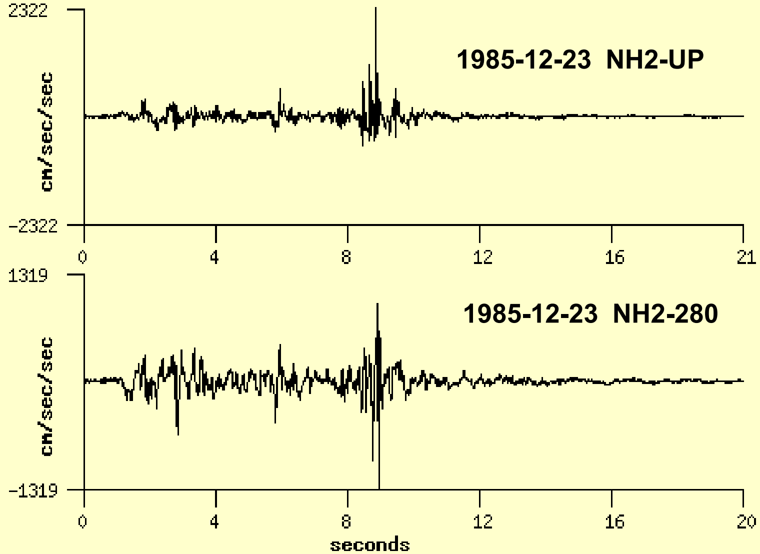

M=6.7 Nahanni EQ, 1985.12.23
R=5-15 km

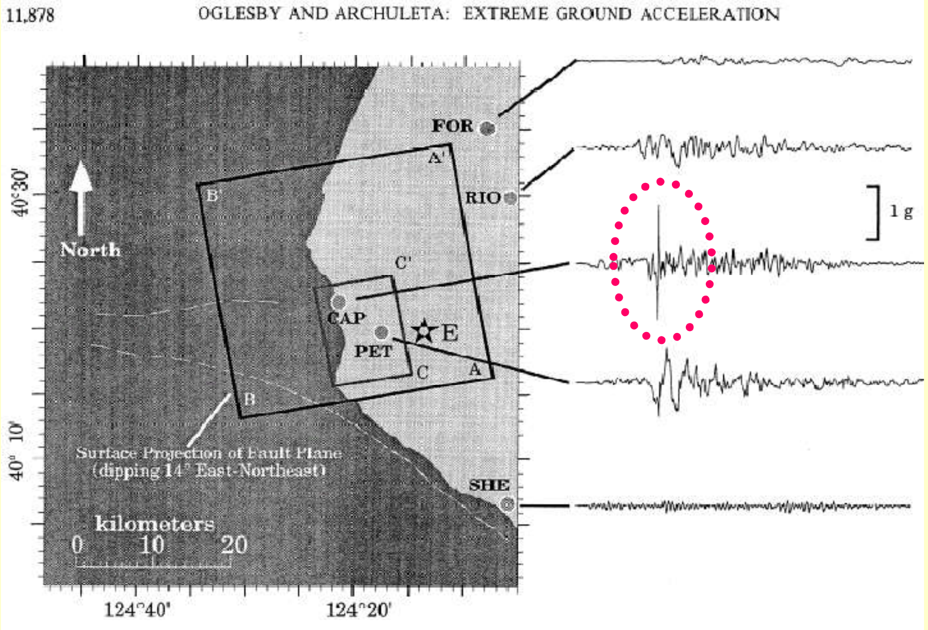

M=7.0 Cape Mendocino/Petrolia
1992-04-25

Probable cause of spikes:

failure of several very strong and localized "strength asperities"

Probable cause of the spike at CAP:

formation, by chance, of an arcuate segment of rupture front, with specific space-time geometry that resulted in powerful constructive interference at CAP

Possible mechanisms of formation of heavy tailed statistics of HF signal (acceleration spikes)

Mechanism A: failure of strong spots on the fault (strength asperities); high local stress drops. Must be related to heavy-tailed slip/slip rate distribution

Mechanism B: occasional formation of correlated/coherent features of the rupture front, making significantly enhanced amplitudes.

Mechanism A+B: formation of correlated/coherent features of the rupture front through interaction of this front with strength asperities

3. Weak or absent HF propagation-related directivity: *isoseismals*

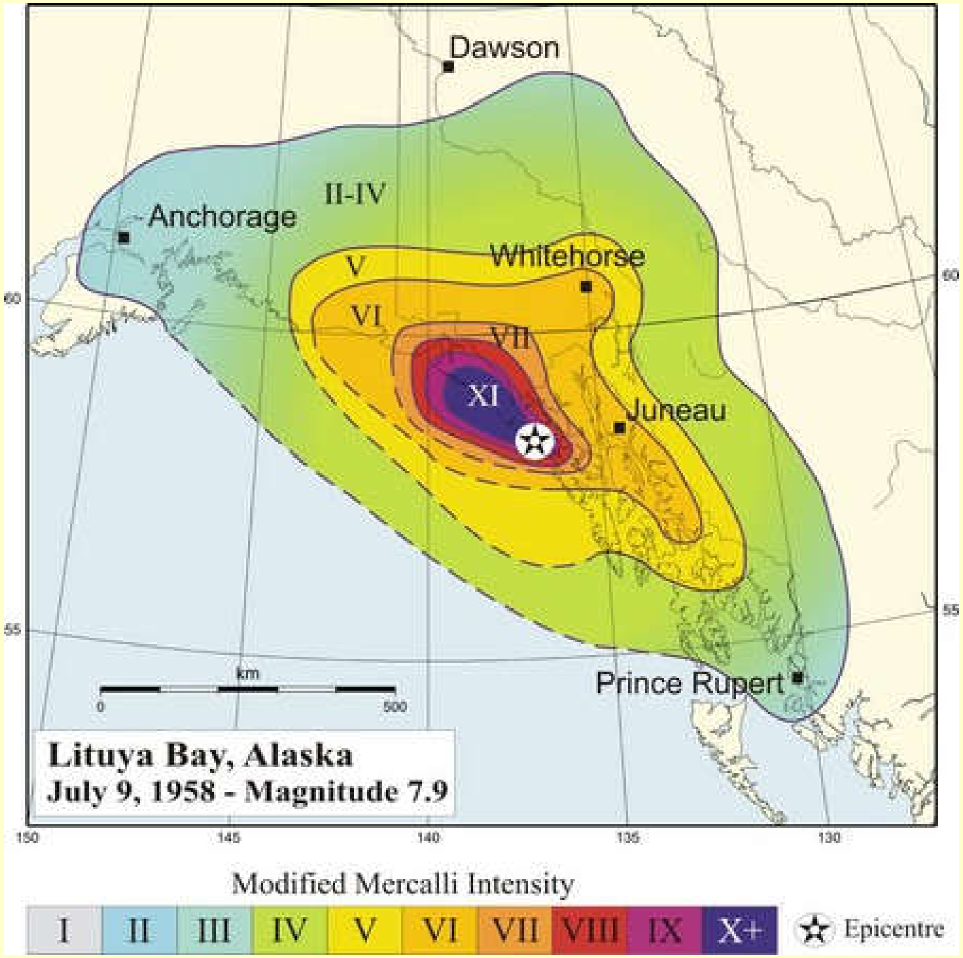

Here, *I*=9+ zone is the rupture area and its vicinity, it gives an idea of the source position. Rupture propagation was unilateral as seen from the position of the instrumental epicenter.

Meanwhile, *I*=5-6 isoseismals show effects of regional propagation.

For this mostly linear source with unilateral rupture, no unilateral pattern is seen in regional macroseismic effects; no clear source-related HF directivity is seen

asymmetric isoseismal shapes are mainly related to lateral variations of attenuation and site effects

Period/frequency dependence of the average directivity factor

that represents by angular dependence of response-spectral acceleration RSA (RSA being comparable to the peak of filtered acceleration)

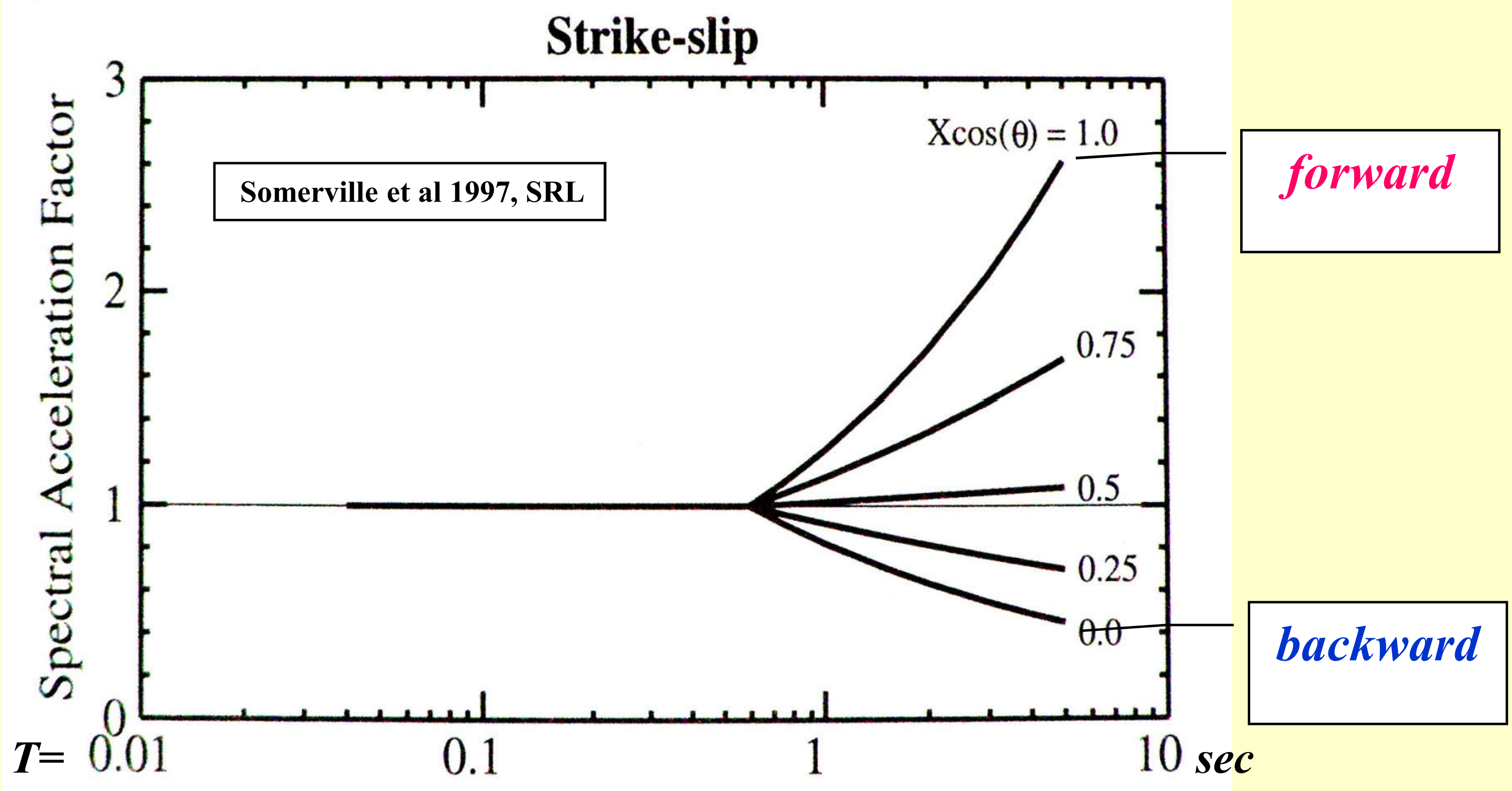

f= 100 10 1 0.1 Hz

Xcos(theta):

X measures degree of unilaterality

(0 for bilateral)

theta is anglular deviation from

forward direction (0 to 180)

Conceptual broad-band fault models and related directivity

Model	degree of incoherence/directivity	
1. Deterministic crack tip; continuous rupture front with well-defined rupture-velocity vector	coherent source; high directivity *HF directivity too high* *LF directivity adequate*	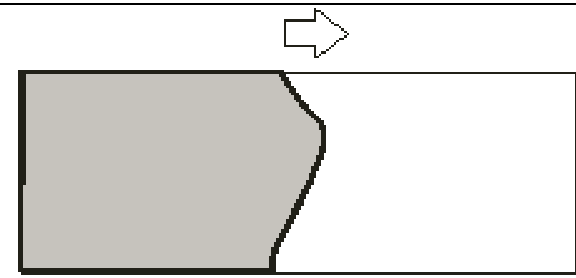
2A. Composite-crack model: small abutting cracks switch on in correlated but not accurately synchronized order; no continuous slip rupture front is virtual;	source is incoherent at HF; marginal directivity at HF *HF directivity realistic* *LF directivity adequate*	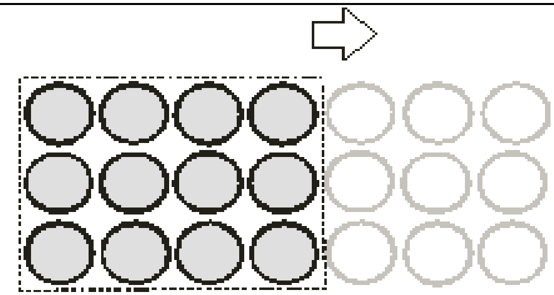
2B. Multi-asperity model: many small strength asperities that switch on in a random still correlated order; rupture front is virtual	source is incoherent at HF; marginal directivity at HF *HF directivity realistic* *LF directivity adequate*	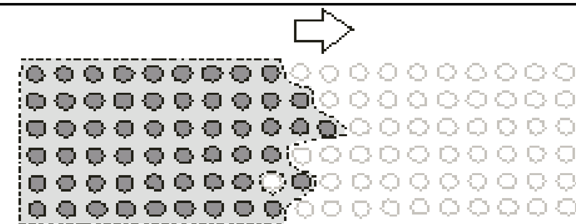
3. Discontinuous, fractal rupture front with tortuous and fragmented geometry; ***no artificial subsources assumed***	source is incoherent at HF; marginal directivity at HF *HF directivity realistic* *LF directivity adequate*	

Example fractal front evolution

(example is based on pure kinematic generator of discontinous front positions; the front “propagates” from left to right, and lighter color codes later rupture time)

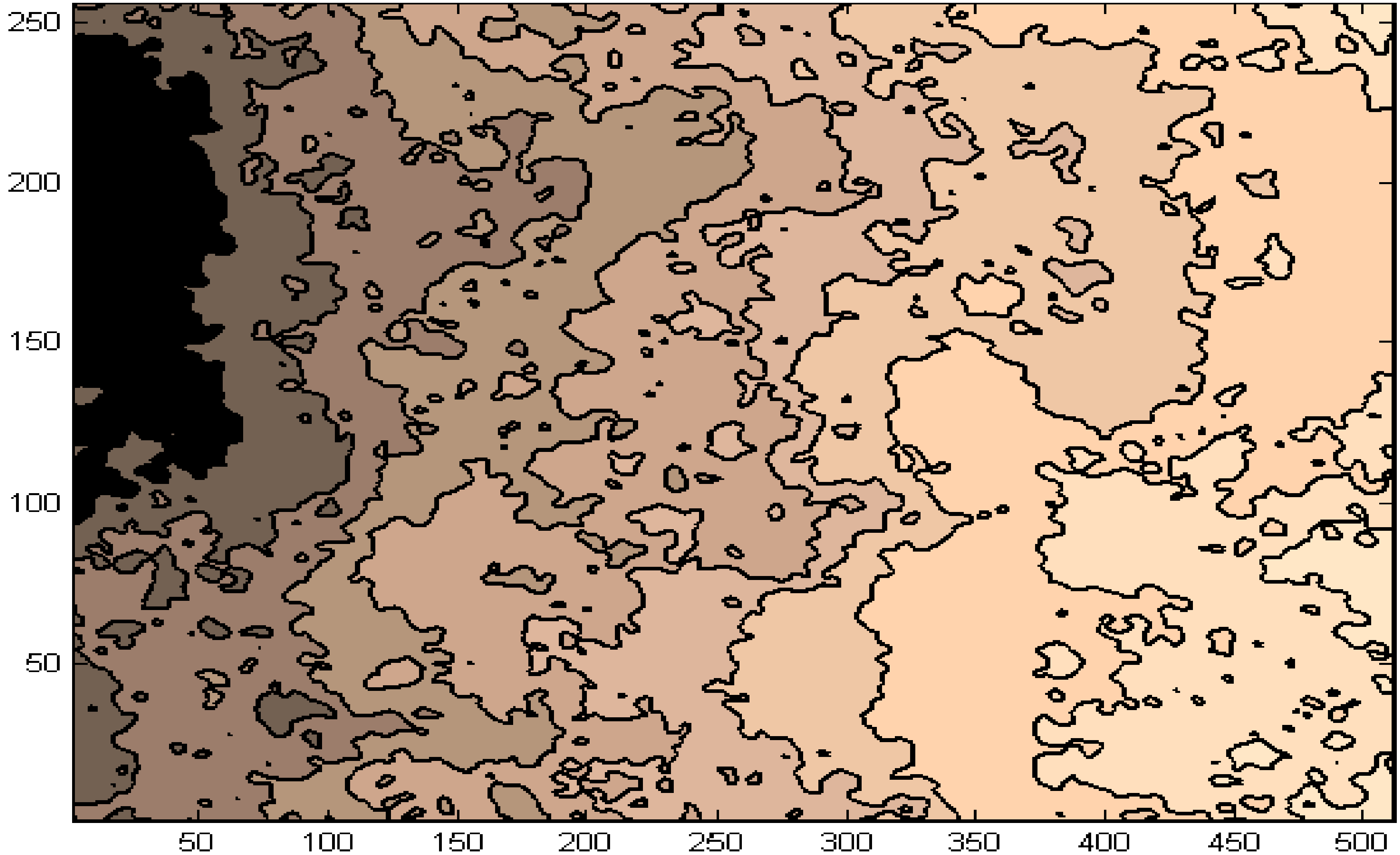

local delay values random with upper bound (uniform pdf) and added trend; power-law spectral exponent -1.4

Simulated quasistatic crack propagation through material governed by discretized "continuum damage mechanics" [Silberschmidt , 2000)]

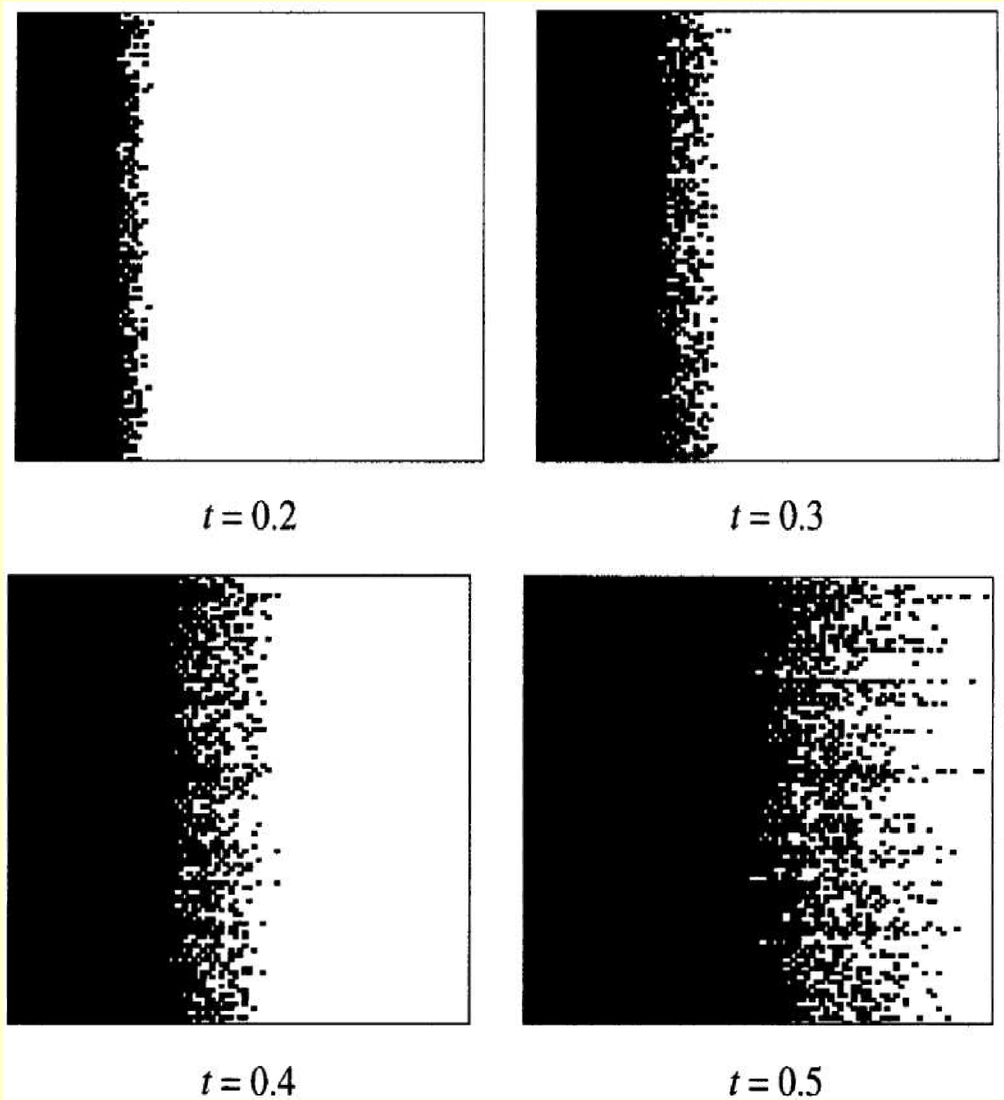

4. The puzzle of f_{max}

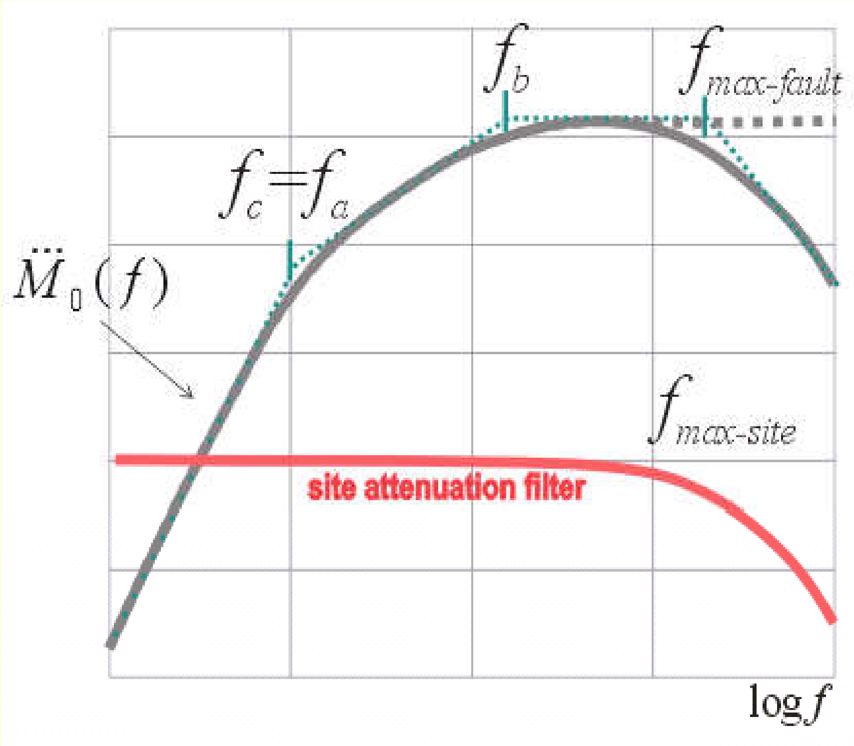

Hanks 1980: f_{max} exists

Aki 1981: f_{max} fault-controlled!?

Anderson&Hough 1984:

f_{max} site-controlled!!

=> kappa [attenuation]

Problem: site-controlled f_{max} effectively masks fault-controlled f_{max} ;

can one find out whether it exists?

(1) find rare cases with ***unusually low*** fault-controlled f_{max}

(2) use records made in (deep) boreholes

Source-controlled *f*-max: low *f*-max examples

Magnitudes 7-7.5
Pairs of earthquakes recorded at the same station
One of the two events have unusually low source-related $f_{max} \approx 3$ Hz
Attenuation-related f_{max} is present as usual
Can be eliminated by analyzing spectral ratio

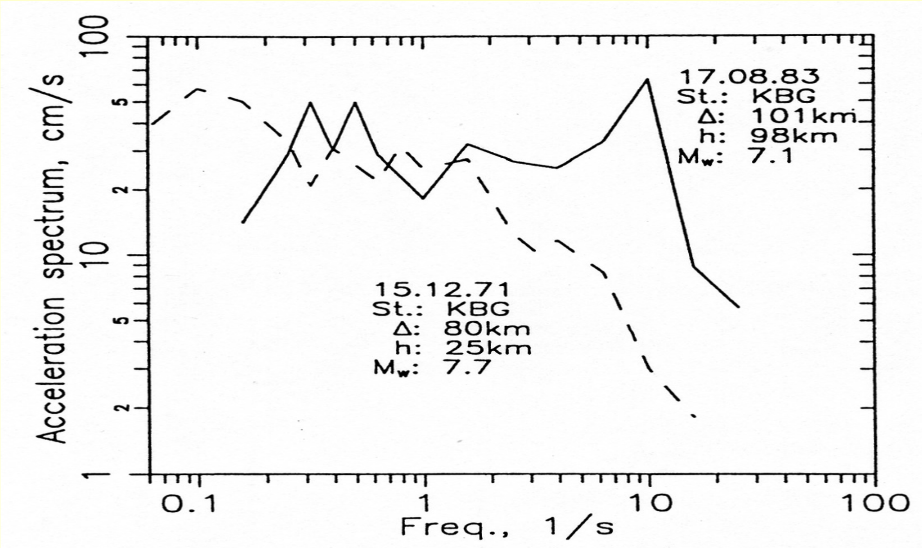

Gusev a.o. 1997

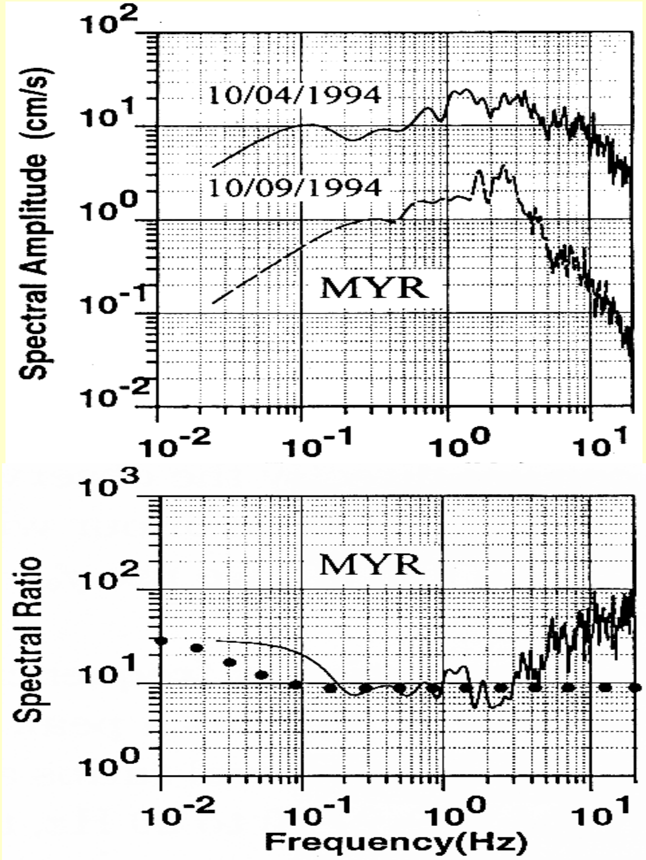

Sasatani 2001

Source-controlled *f*-max: deep borehole examples

Low to moderate magnitudes
Instruments in deep boreholes,
eliminated site-(attenuation)-controlled f_{max}
Found, typically: source-related f_{max} between 10 and 25 Hz,

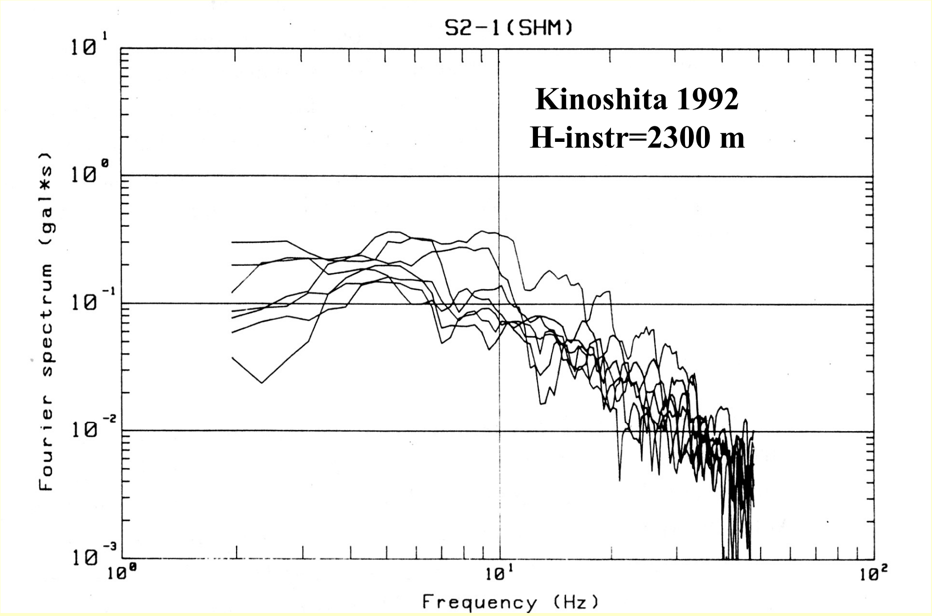

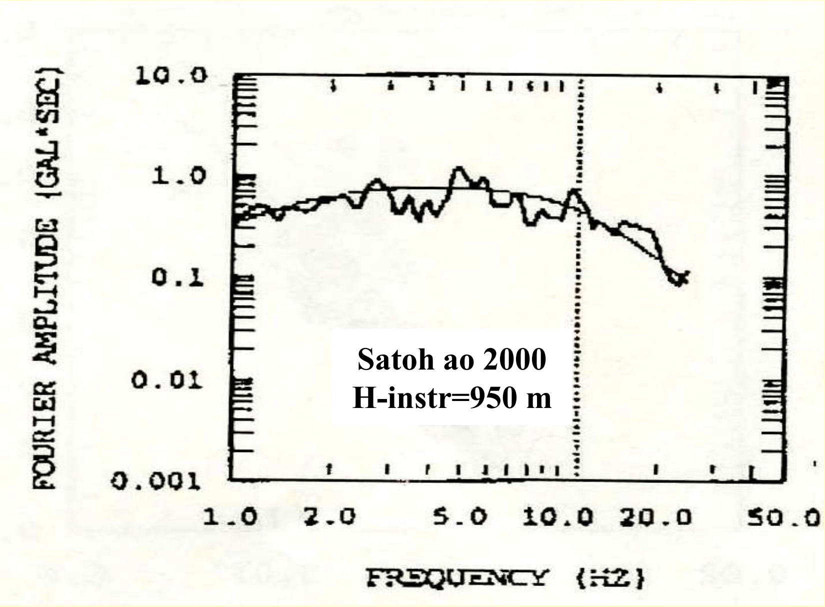

Source-controlled *f*-max: systematic study using KIK-net data (Tsurugi et al 2008)

- three large events analyzed
- average spectral ratios are estimated using many aftershocks recorded on many moderate-depth borehole stations
- path-related f-max suppressed

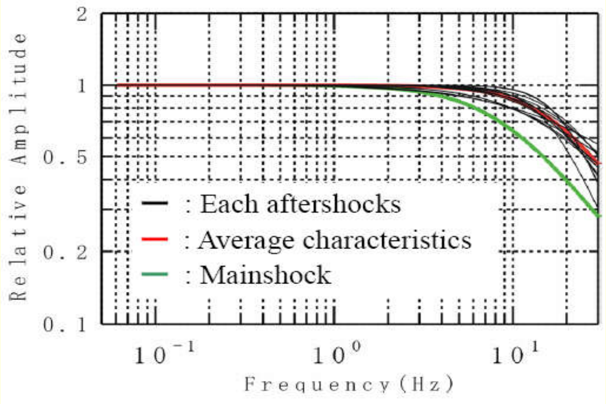

(1)The 2003 Miyagi-ken Hokubu earthquake

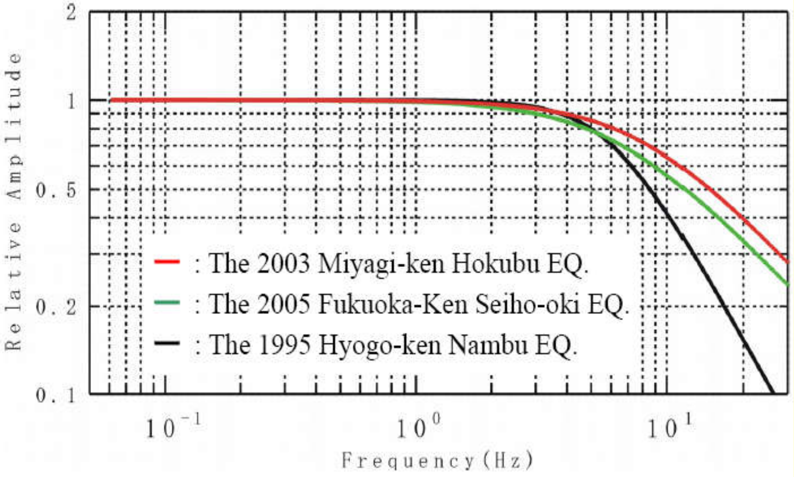

Fig.3 High-cut filter of large event, $P_L(f)$.

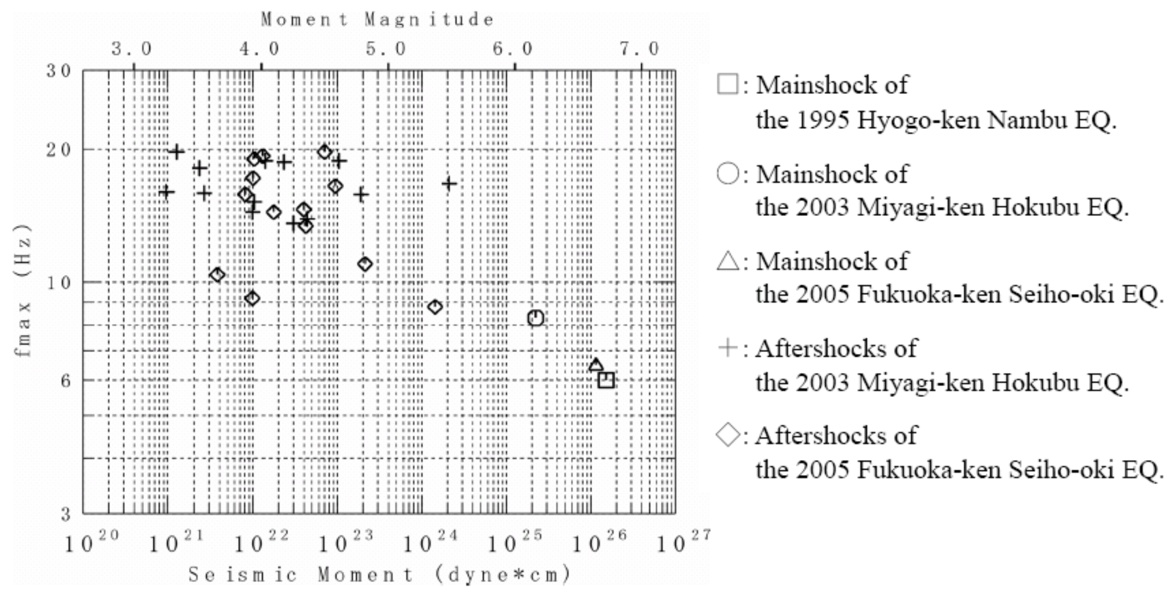

Fig.5 Relationship between seismic moments and f_{max}'s

Source-controlled *f*-max: summary

1. Source-controlled *f*-max seems to be a regular feature of earthquake faults;

   the fact is not 100% established because it is technically very difficult to observe directly

2. Source-controlled *f*-max reflects upper wavenumber limit of rupture front propagation details

3. Slight tendency of *f*-max to decrease with increasing Mo

5. How are related: (1) the distribution of HF radiation capability in space-time over the area of a propagation fault, and (2) similar distribution of local slip rate

Variant 1: **HF energy is generated mostly by large-slip patches, often called "asperities"**

Variant 2: **HF energy does not match high-slip patches;**
Variant 2a: **Rather, HF energy generation is "complementary" to slip**

Sources of information:
1: Degree of correlation between signals: (1) body wave displacement and (2) HF instant power; derived from a record of at intermediate-depth earthquake at the same station,

2. Degree of correlation between space-time distributions of (1)slip/slip-rate and (2)HF radiation capability ("luminosity") as derived from the results of inversion of source structure

Comparing (1) body wave displacement pulse *and* (2) squared HF body wave velocity pulse from the same record of intermediate-depth earthquake

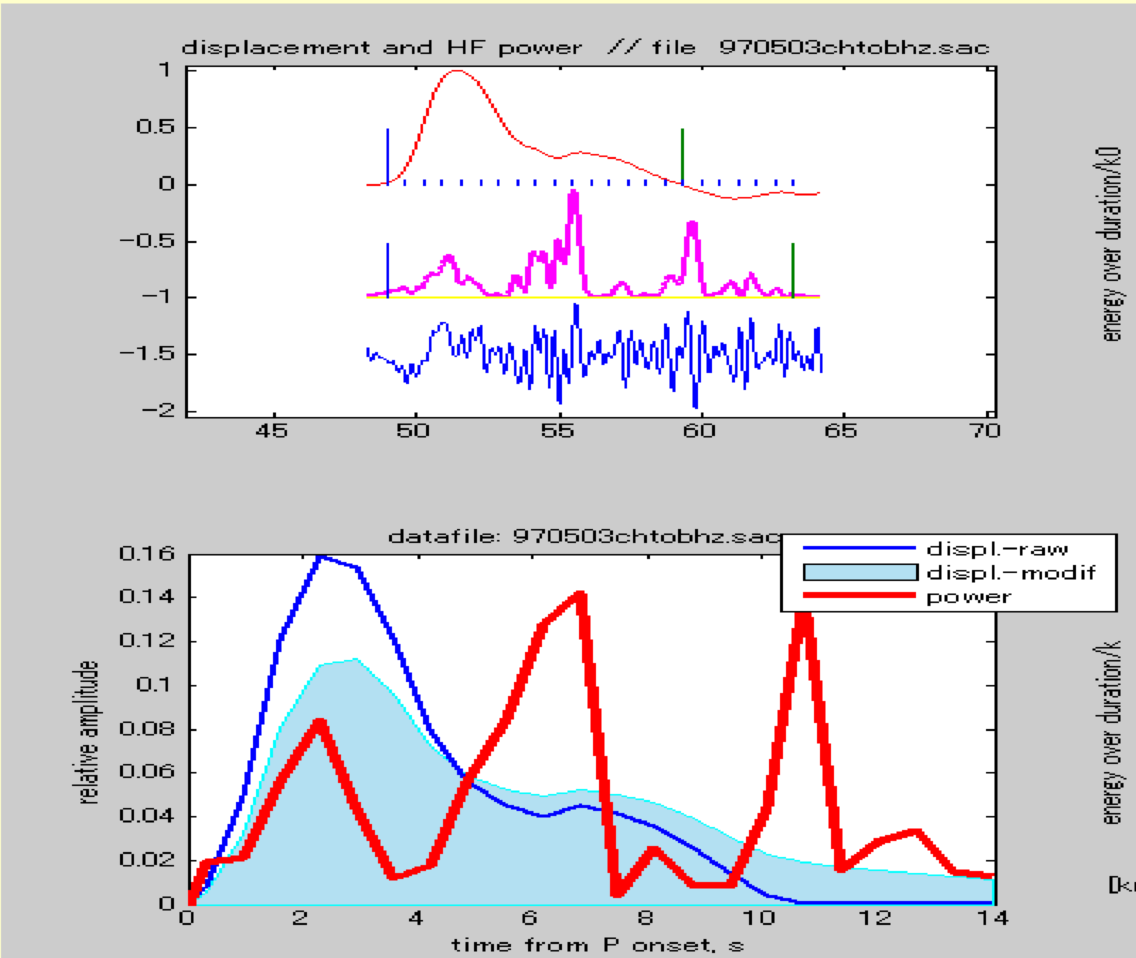

Gusev a.o. (2005) used
251 teleseismic P-wave records of GDSN
from 23 intermediate-focus earthquakes
(h=100-225 km)
with Mw=6.8-7.7.
As a HF signal, we use squared velocity
in the 0.5-2.5 Hz band

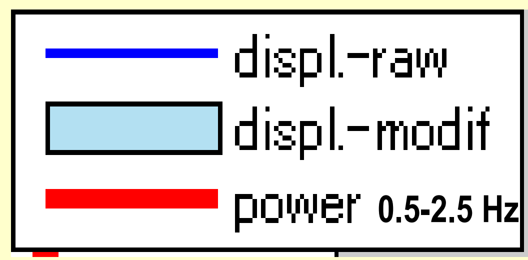

Examples of good and bad correlation between displacement and HF power

low-ρ cases

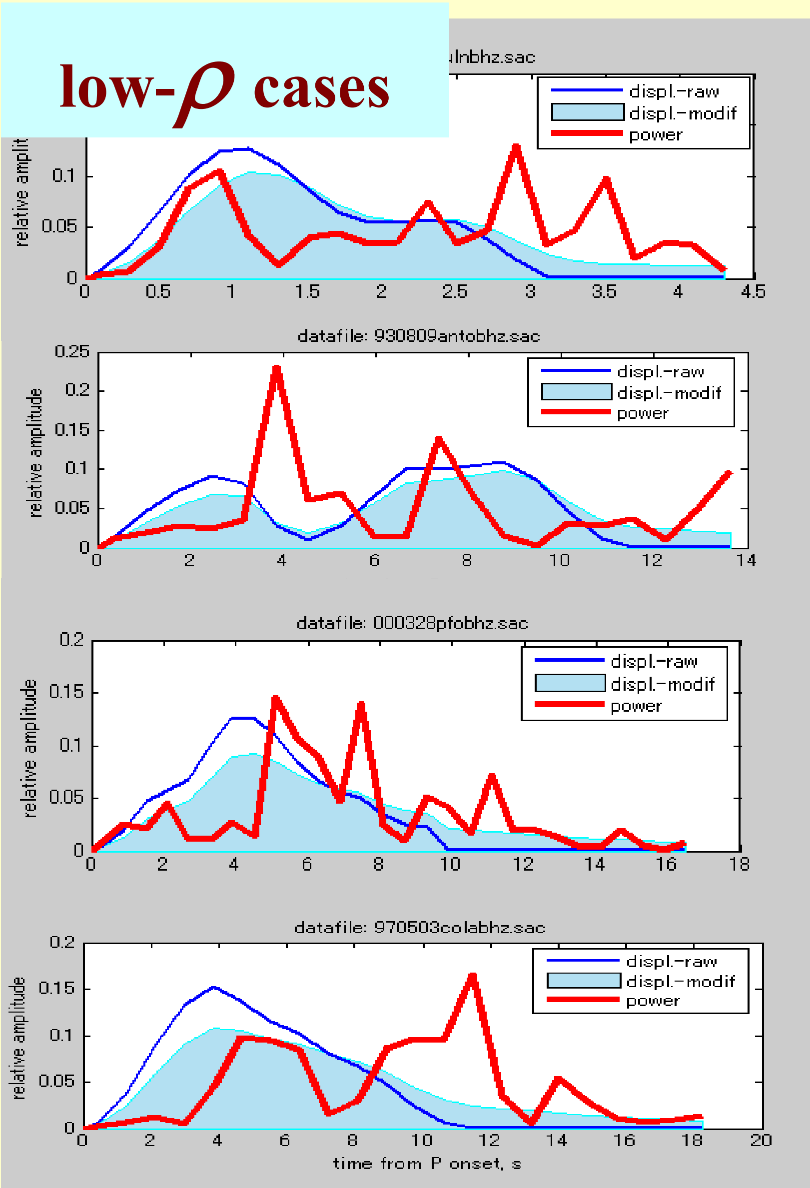

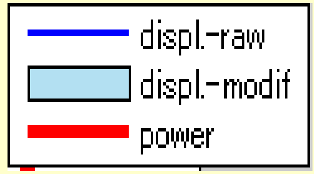

high-ρ cases

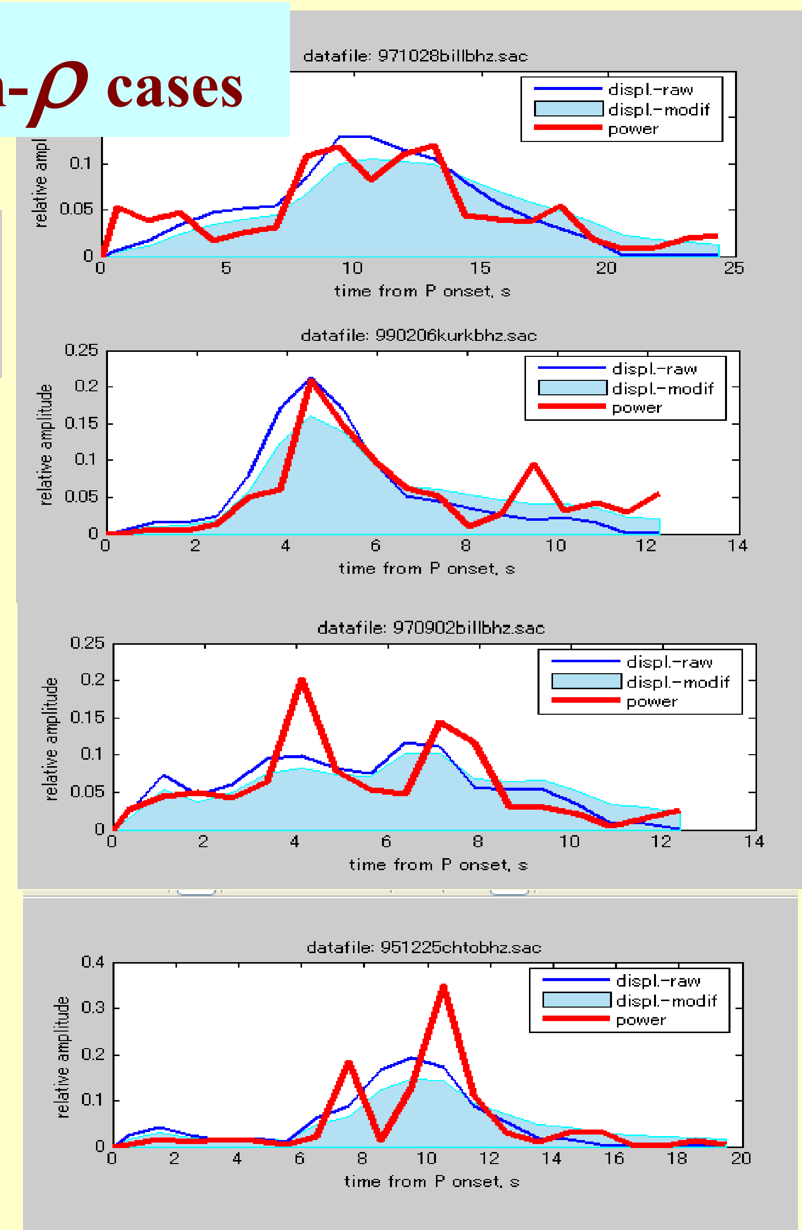

Relationship between local slip and local HF radiation capability -inversion example

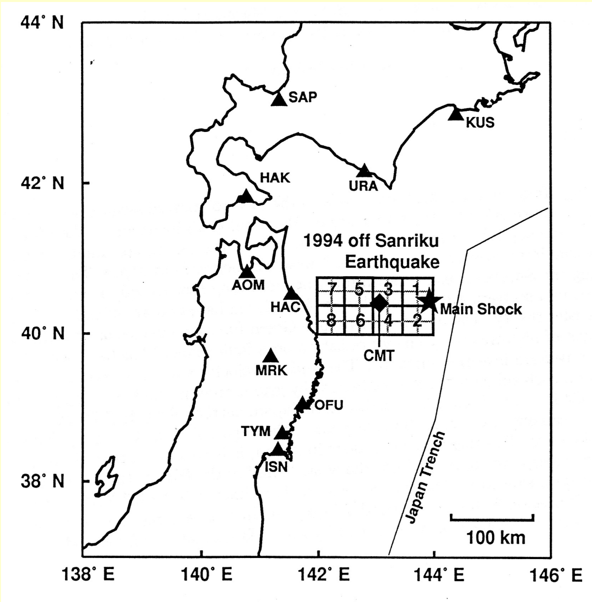

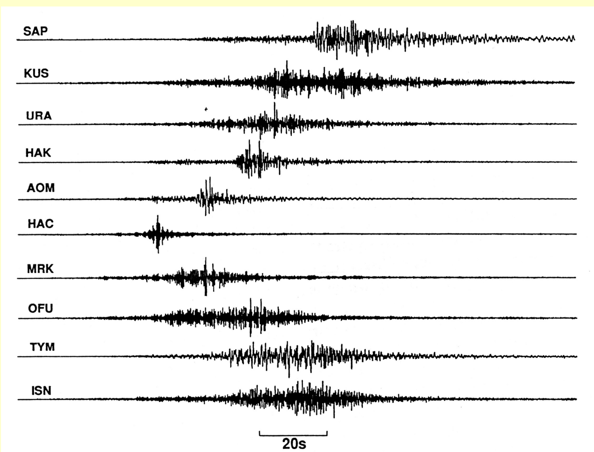

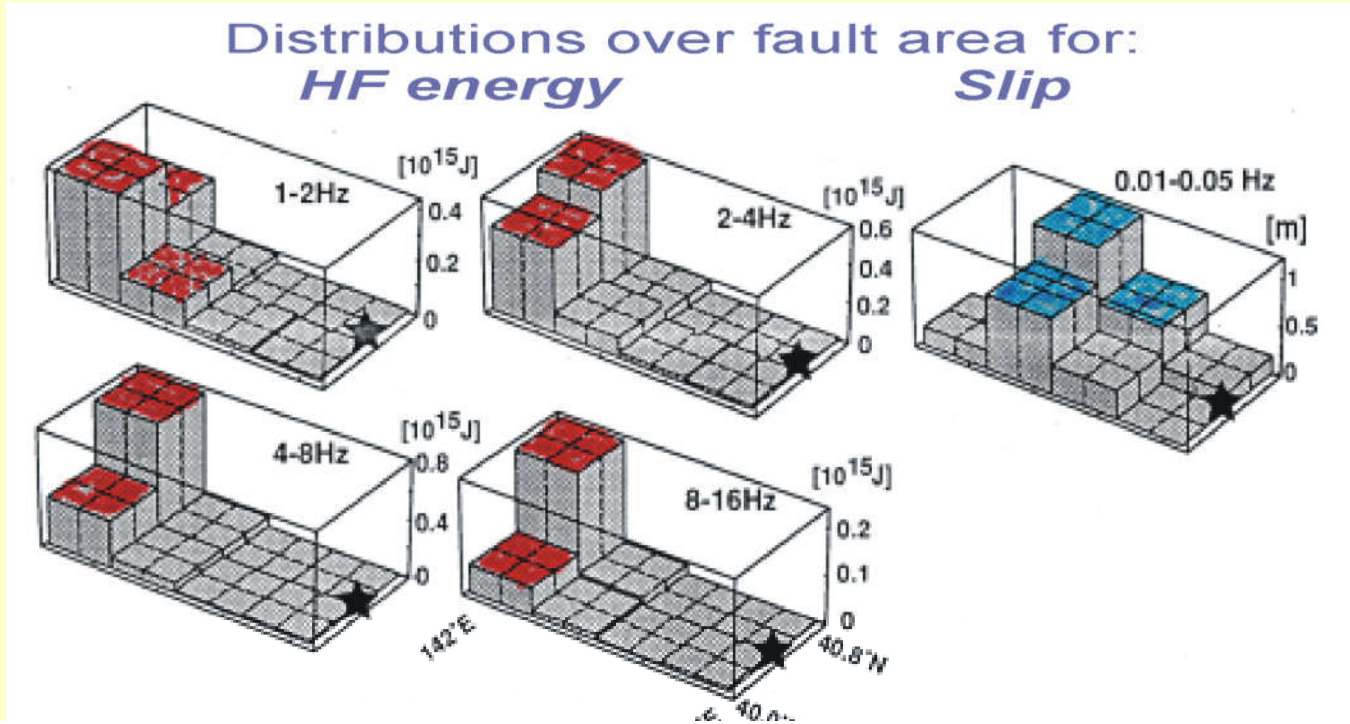

1994, M7.7, off Sanriku, Japan; inverted by Nakahara a.o. (1998)

Summary on slip-HF energy relationship

1. No clear tendency to match between high-slip-rate and high-luminosity areas/time moments
2. “Complementary” behavior is common
3. Coefficient of correlation varies widely, from less than 0.3 to 0.9

6. Stochastic self-similarity of envelopes of high-frequency teleseismic *P*-waves suggests fractal pattern for earthquake rupture

band-filter **square, set window** **smooth**

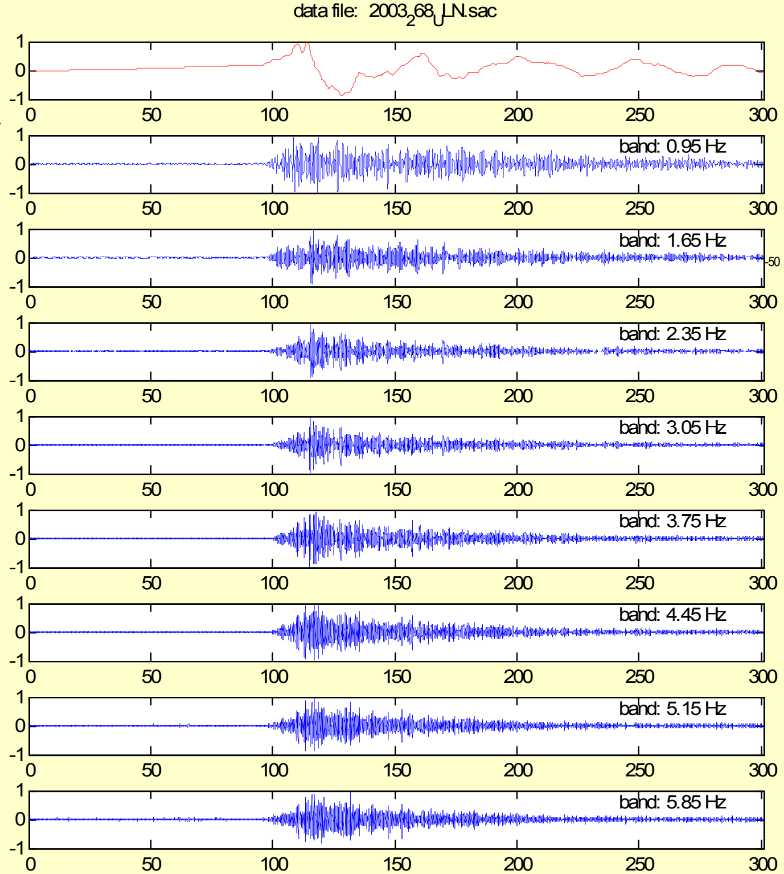

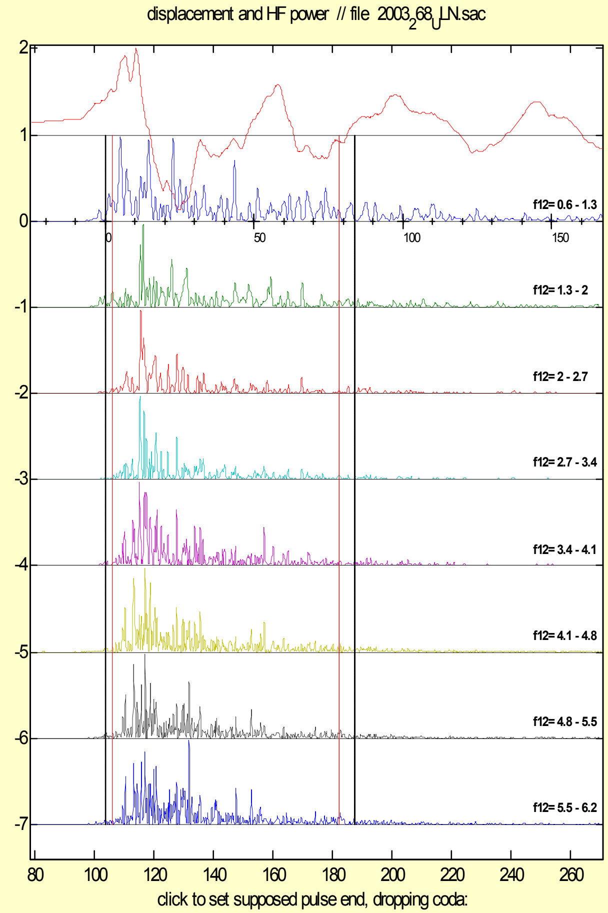

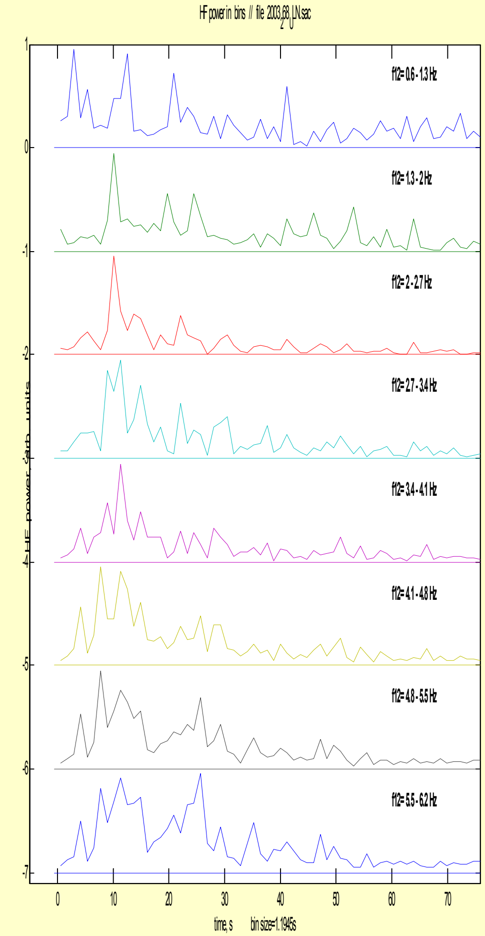

2003.09.25 *M*=8.1 Tokachi-oki earthquake at ULN

Calculate variogram, find $2H=d\log V/d\log\Delta t$
Calculate power spectrum PSD(f); MCPSD(f), find $\alpha=d\log PSD/d\log f$; $H(\alpha)=\alpha/2+0.5$

$\log_{10} V(\Delta t)$

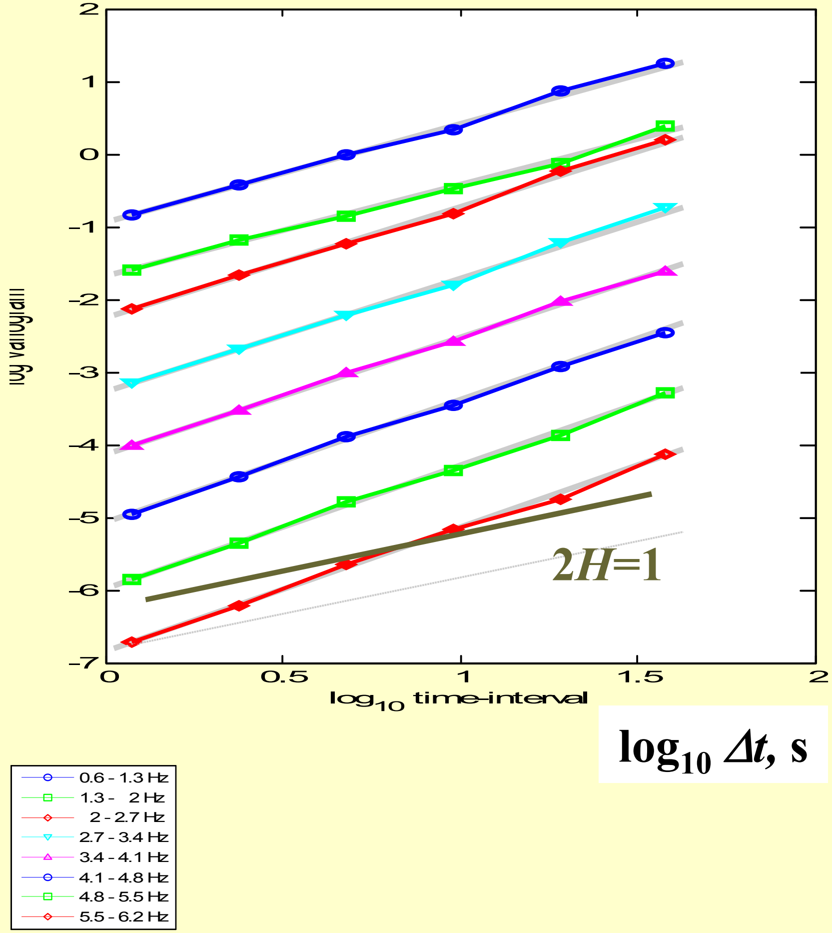

$\log_{10} \Delta t$, s

$\log_{10} PSD(f)$
$\log_{10} MCPSD(f)$

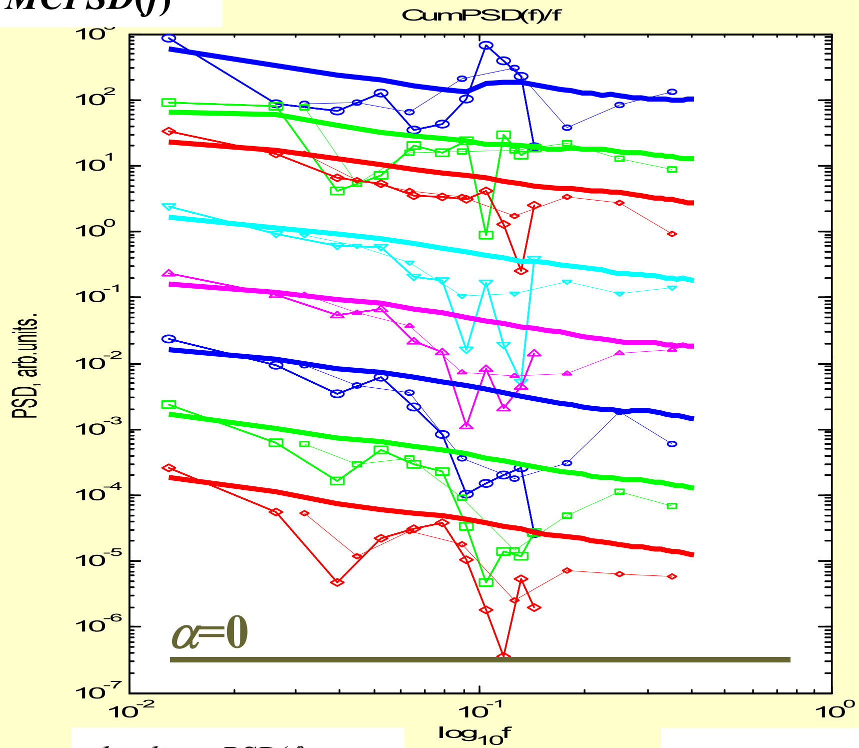

thin lines:PSD(f)
thick lines: MIPSD(f)

$\log_{10} f$, Hz

MORE EXAMPLES

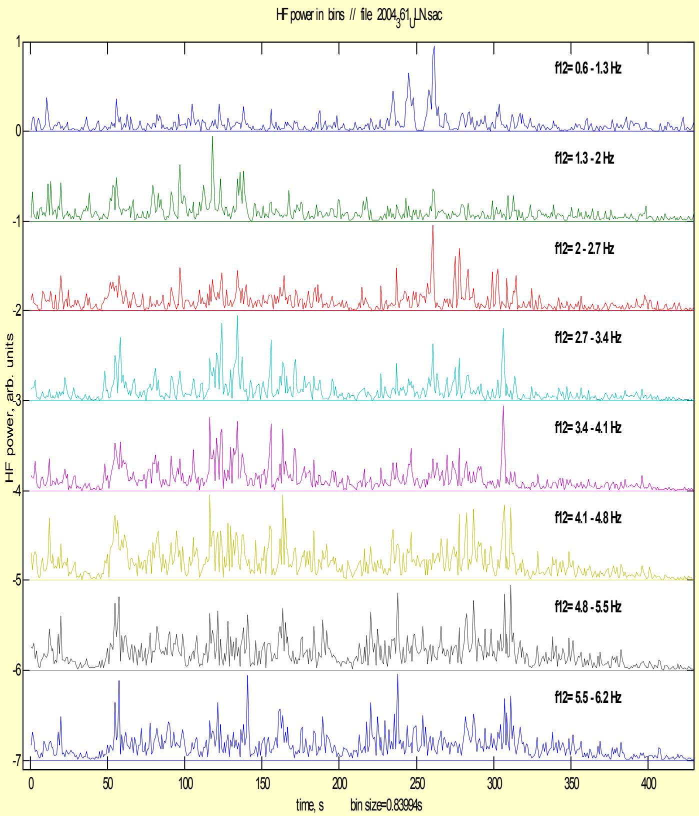

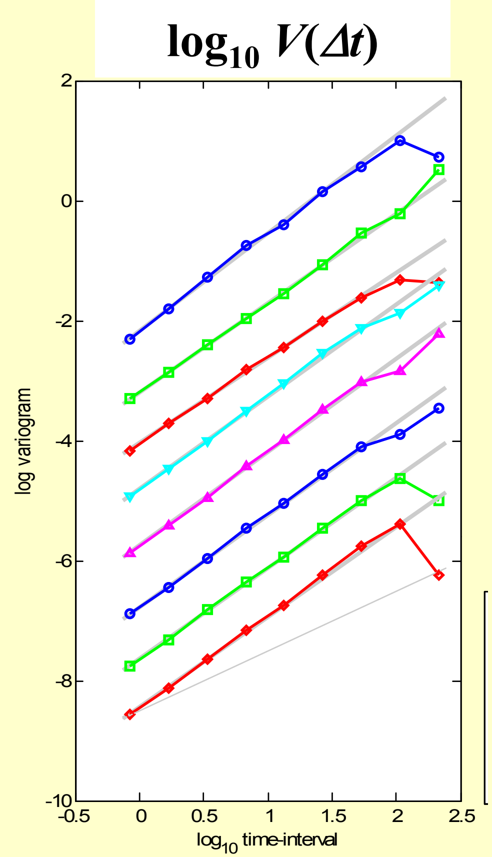

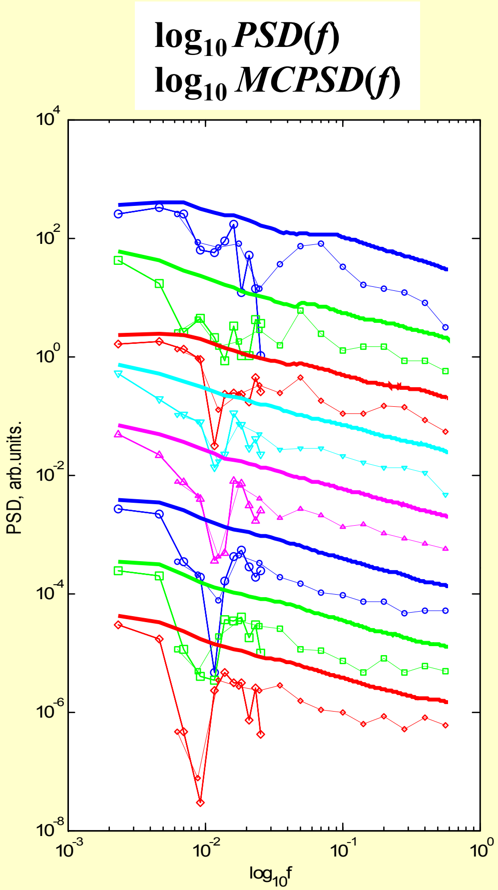

Data: 2004.12.26 M=9.2 Sumatra earthquake at BHZ channel of ULN

Estimates of H and α for each event, averaged over 8-30 records and over 8 frequency bands

Date	M_w	Region	Type[1]	no records N/N_{min}[2]	H	$\sigma_{ir}(H)$	$H(\alpha)$	$\sigma_{ir}(H(\alpha))$	α	$\sigma_{ir}(\alpha)$
19971205	7.9	Kamchatka	*Su*	19/7	**0.75**	0.07	**0.82**	0.05	**0.63**	0.09
19980325	8.2	S.Pacific	*Cr*	8/2	**0.79**	0.03	**0.83**	0.04	**0.66**	0.08
20021103	8.4	Alaska	*Cr*	17/6	**0.71**	0.06	**0.83**	0.05	**0.66**	0.11
20030925	8.2	Hokkaido	*Su*	18/10	**0.78**	0.05	**0.82**	0.05	**0.63**	0.09
20041226	9.2	Sumatra	*Su*	32/21	**0.75**	0.07	**0.80**	0.05	**0.60**	0.09
20050328	8.7	Sumatra	*Su*	20/11	**0.80**	0.04	**0.82**	0.04	**0.64**	0.10
20060420	7.6	NE Russia	*Cr*	28/4	**0.72**	0.08	**0.78**	0.07	**0.56**	0.14
20061115	8.1	Kuriles	*Su*	14/7	**0.74**	0.05	**0.80**	0.05	**0.60**	0.11
average					**0.76**	**0.063**	**0.81**	**0.053**	**0.62**	**0.010**

σ_{ir} –inter-record rms deviation

[1]Tectonic kind of a fault: subduction(*Su*) or crustal (*Cr*)

[2]Total no of records used and no of usable records for higher-frequency bands

Self-similarity imprint can also seen for HF instant power of most of accelerograms, for M=6.5⁺ and Δ=0-100 km

1952, M7.5, Kern county, California
Taft , S69E

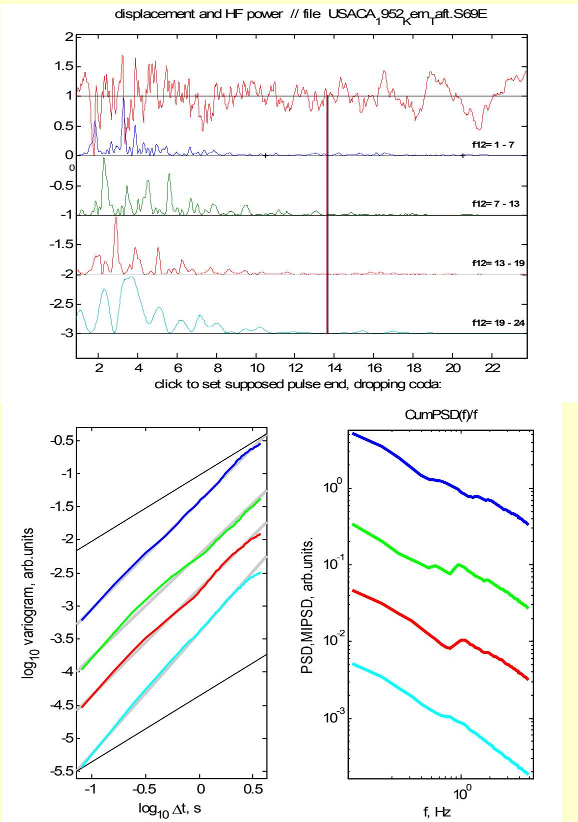

1965, M6.7, Puget Sound, Washington state, USA
Fed.Off.Building, S32E

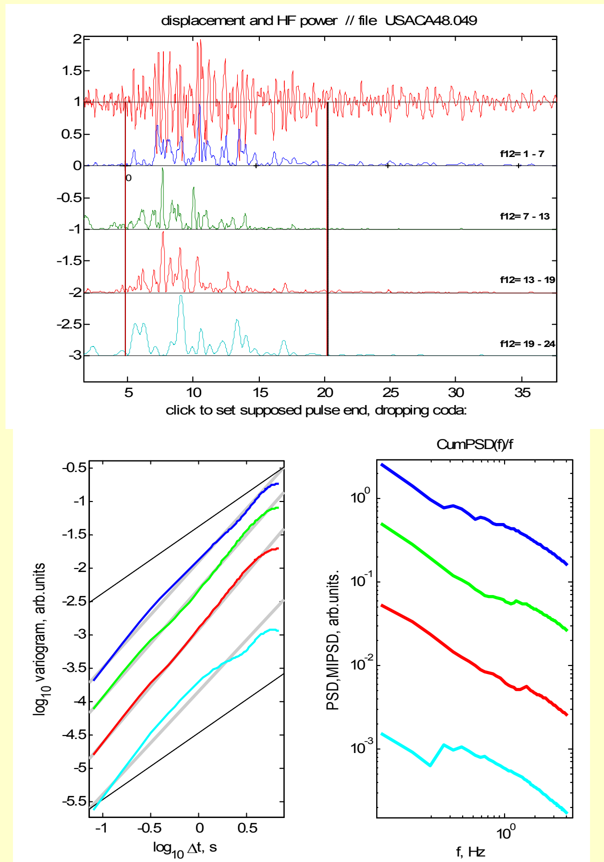

1972, M7.2, Hawaii
Hilo, UH; N74E

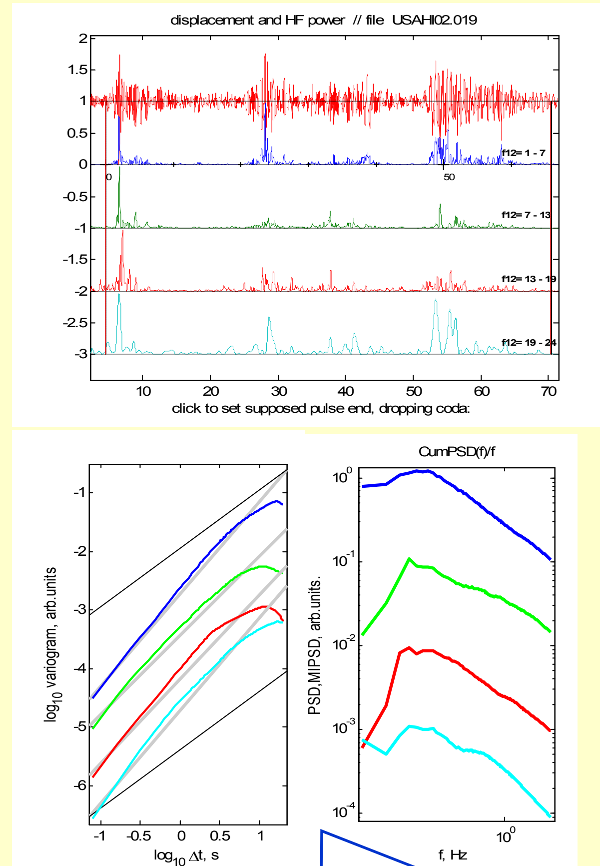

in all examples:

“Band-limited” self-similarity only :
within the period range T=0.05-3 s

Fractal HF envelopes – a summary

1. Propagating earthquake rupture produces random-looking HF (1-20 Hz) radiation with self-similar correlation structure of instant power
2. This fact suggests that earthquake rupture process is multiply-scaled, with fractal features

   (and cannot be reduced to smooth brittle crack propagation with 1-2-3 characteristic scales)
3. Multiple-scale tendency for instant power of band-filtered signals is much more systematic as compared to the well-known multi-scaled tendency over may bands, namely “omega-square” spectral model
4. Checking self-similarity of HF wave envelopes may provide an important test to verify how realistic are simulated earthquake sources models

Part B. A possible mechanism responsible for properties of HF radiation (partly)

The discussed mechanism is the generation of multiple-scaled heterogeneity of strength and local stress drop

by randomly non-planar, rough, multiscaled

NON-CONTINUOUS fault geometry

Strength heterogeneity from random fault wall relief (1):

model with fault gap formation

fault strength is concentrated at pressed patches/strength asperities [black, 10%]

free space/gap is formed with negligible strength [grey, 90%]

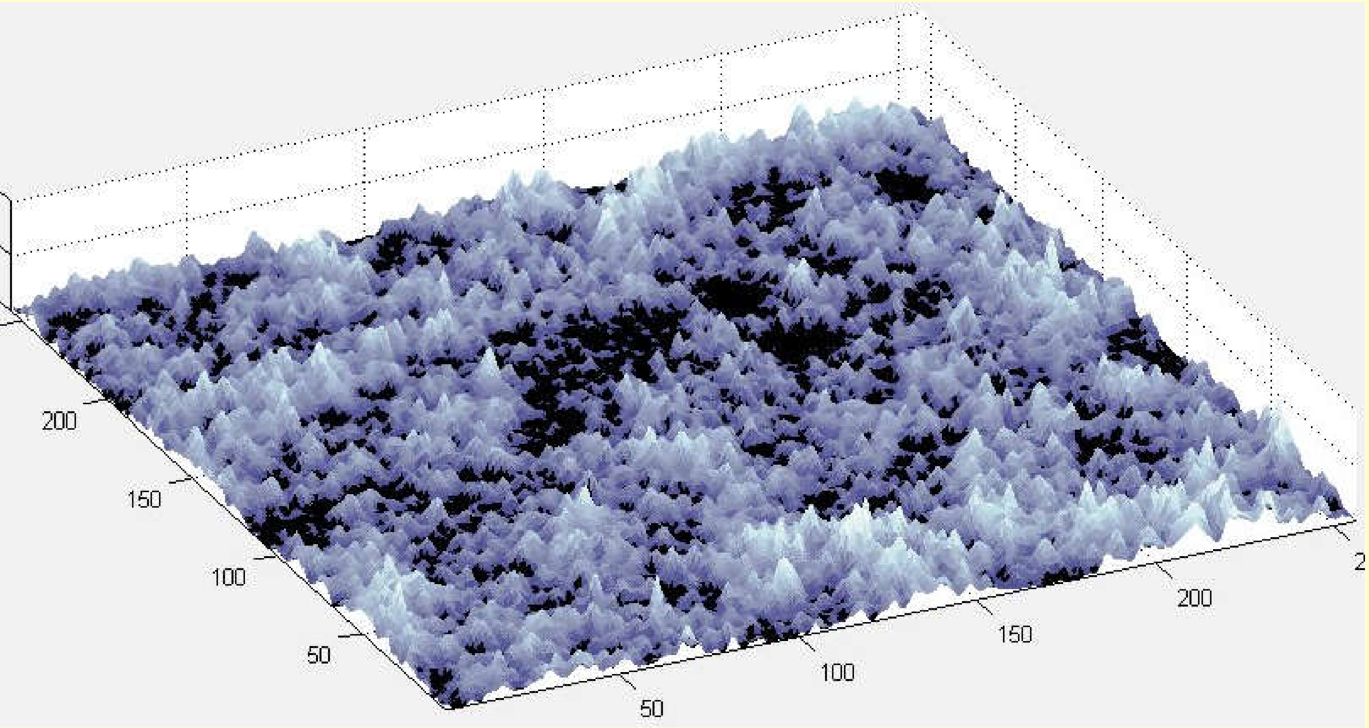

3D composite topography of fault walls contacts: black plains where gap=0 all strength localized at "lakes"

Attractive model:

explains:

- randomness of HF signal
- non-Gaussian accelerograms

Difficulty:

needs sufficient pore pressure to create free volume at depth

Strength heterogeneity from random fault wall relief (2)

free-space/gap is closed by confining pressure;
fault walls contact over entire area

Rough, *fractally curved* fault (Dieterich 2000)
with no free space

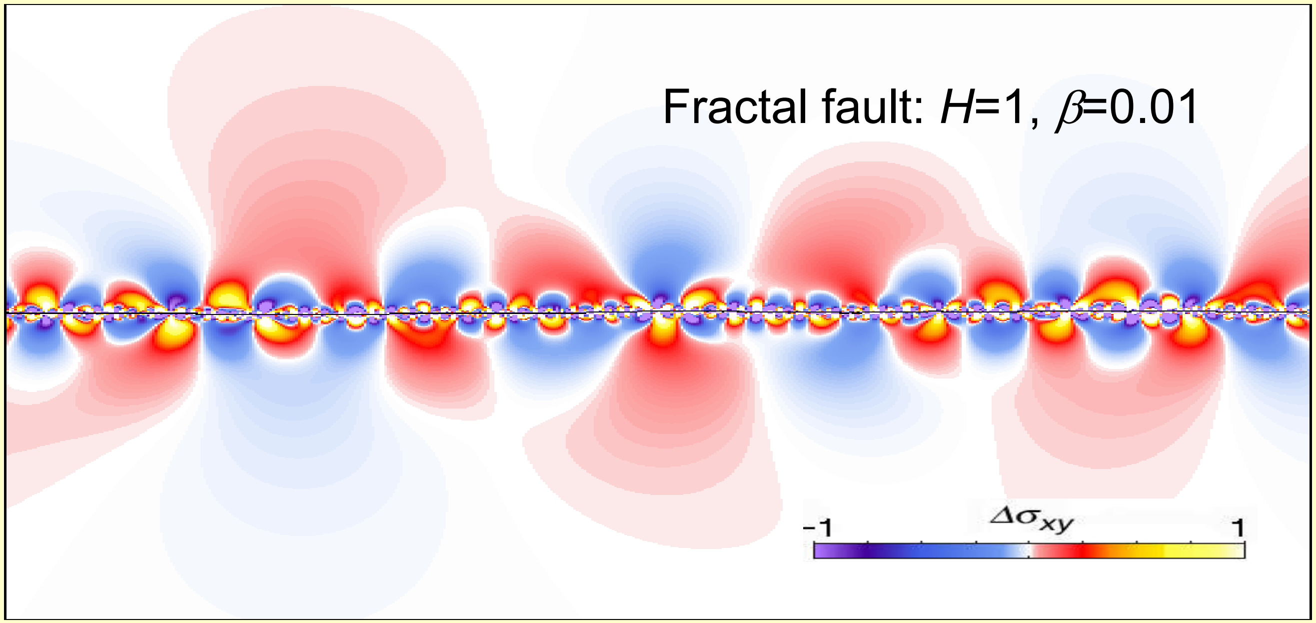

Attractive model:
explains:
- randomness of HF signal
- strong local patches

not so efficient to explain:
- non-Gaussian accelerograms:

Difficulties of strength heterogeneity models based on fault wall relief

Along a rough geological fault slipping in geological time, both
(1) stress concentrations and
(2) free volume
increase with each earthquake;

Although relaxation of stresses may take place through yielding of material, free volume cannot disappear in this way

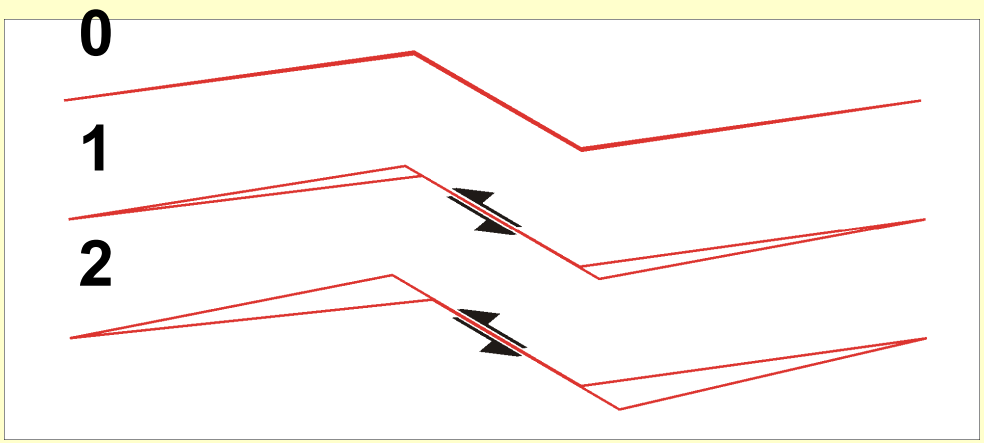

why ***monolithic*** fault walls are impossible

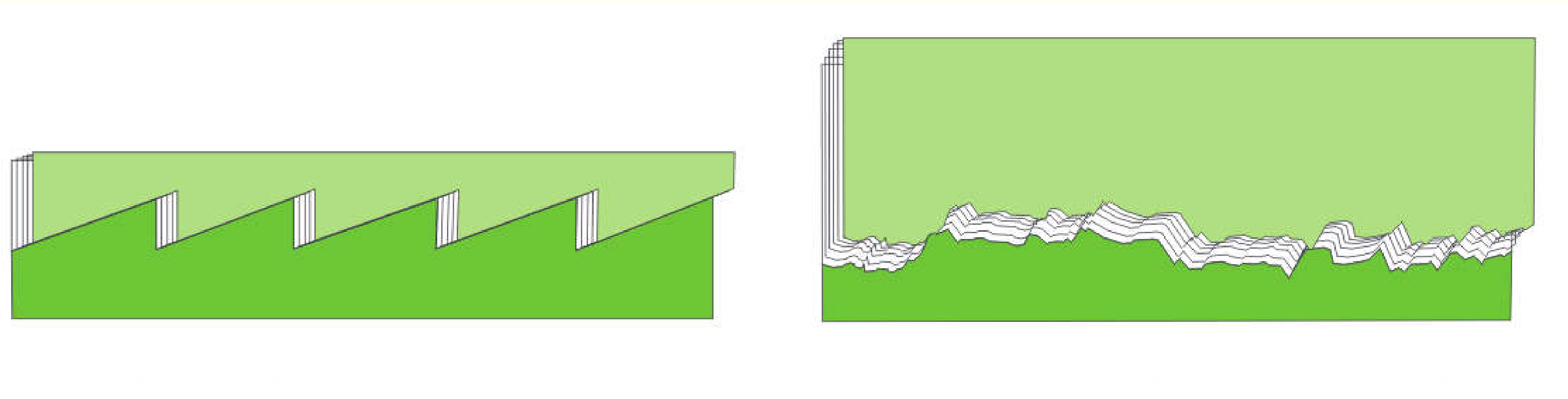

For a random fractal profile with realistic parameters, in geological time average gaping grows proportionally to slip,

like for a deterministic periodic saw-tooth profile;

but with no upper limit because longer and longer periods of the profile become active

Endless free-volume accumulation around a fault can be suppressed by assumption of *non-monolithic* non-planar fault walls

Andrews (1994): fault is multiply bifurcating/branching
Medium consists of many discrete monolithic blocks
Stress concentration is strongly suppressed; and gaping formation is limited

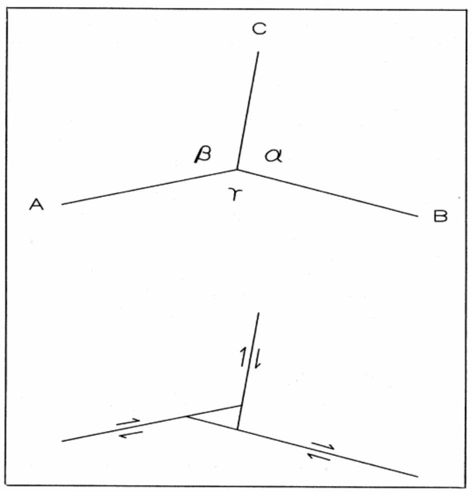

Fig. 1. Top: a junction of fault segments A, B, and C. The opposite angles α, β, and γ are each less than 180°. Bottom: rigid-body displacement at the junction consists of slip in the same sense on the three fault segments, and a void opens.

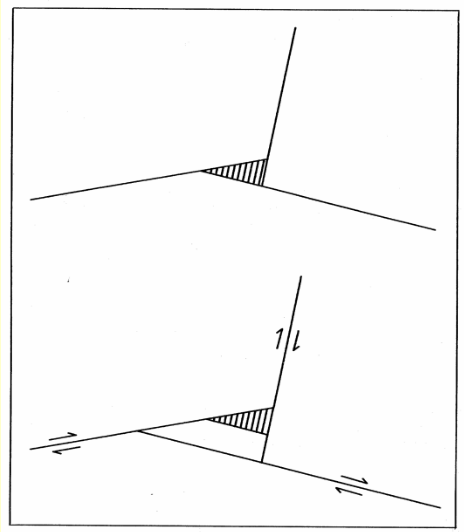

Fig. 4. Top: the triple junction shown in the bottom of fig. 1 with the void filled with fluid or remineralized. Bottom: another increment of slip produces a larger increment of void volume.

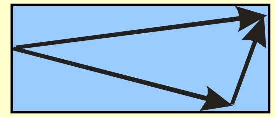

Attractive model:
explains how stress concentrations can relax and disappear from a rough surface of a sliding fault

Never was sufficiently developed to show its real potential;

Problem: mechanics of finite slip and related stress relaxation not developed

no single fault gap; *branch faults* at each main-fault turn; secondary small gaps are formed
no strong stress concentrations related to fault shape
splitting of dislocations pumps a fraction of seismic moment to branch faults
strength still highly heterogeneous because finite amount of slip is incompatible and fresh material must be crushed:

Two general ways of sliding along a corrugated fault

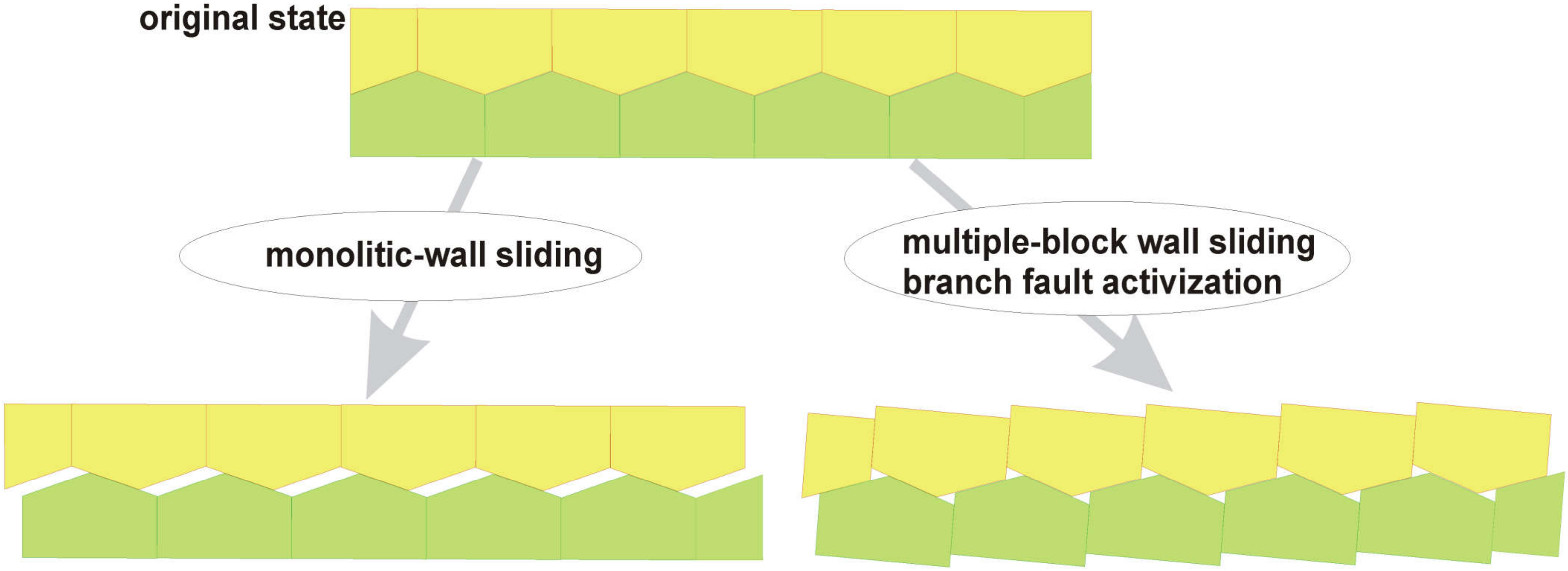

Traditional model:
monolithic walls,
unlimited free space formation

Multiplied *Andrews 1994* model:
walls consist of discontinuous blocks;
free space formation: minimal;
significant problem: *TWIST*

other multiple-block sliding models possible

Sliding along a corrugated fault: the case *Andrews 1994* continued, rigid blocks

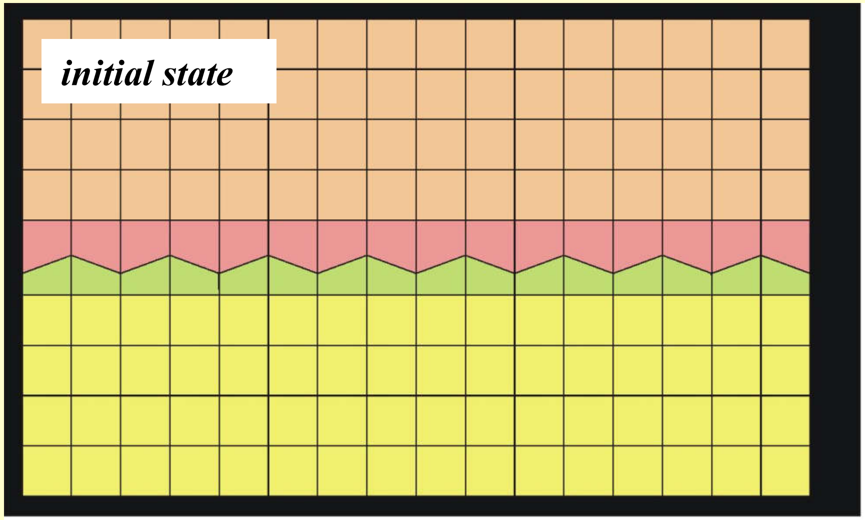

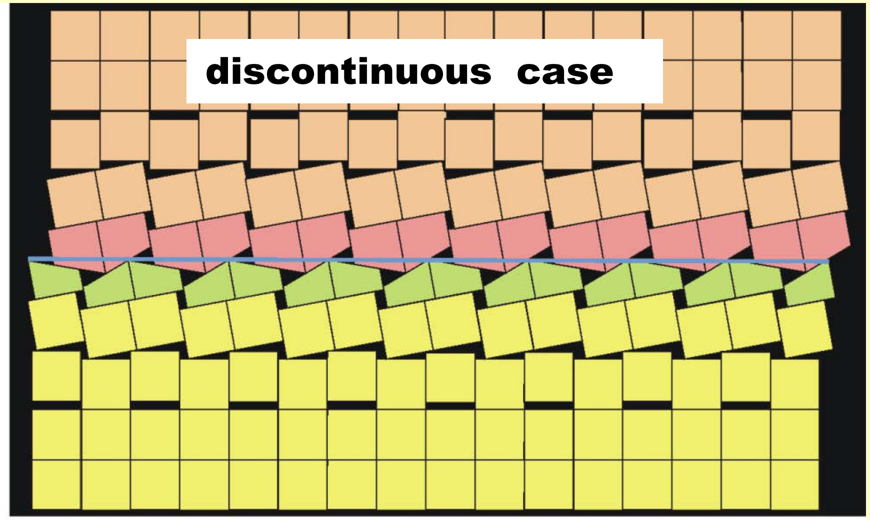

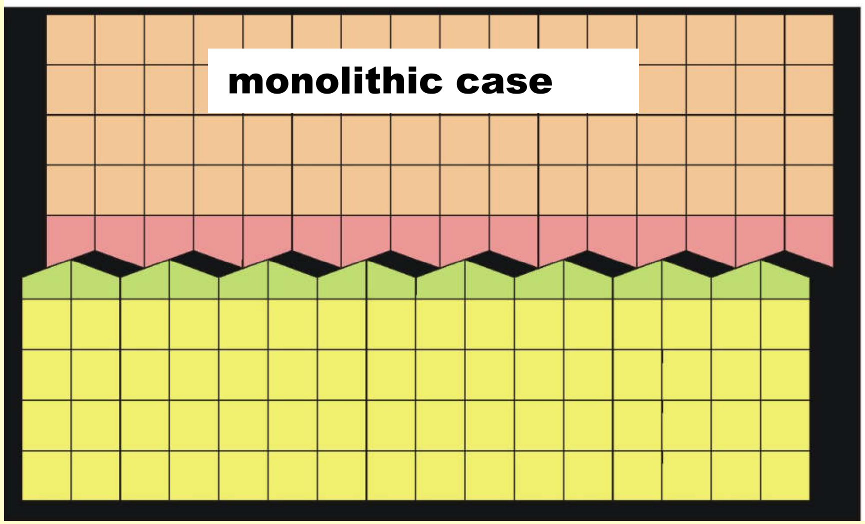

Assuming *Andrews 1994* faulting style for blocks of fault walls in immediate contact, one has to introduce two dilatant layers of twisted blocks that provide the match between rotated near-fault blocks and non-distorted half-spaces at a distance. This twist needs significant increase of free space. This additional free space is much above one needed in the “monolithic” case. Therefore, this mode of discontinuous faulting is doubtful.

Sliding along a corrugated fault: no block rotation, rounded blocks

case 1: excess and deficit of material separately transported to a boundary of elastic volume; no local compensation

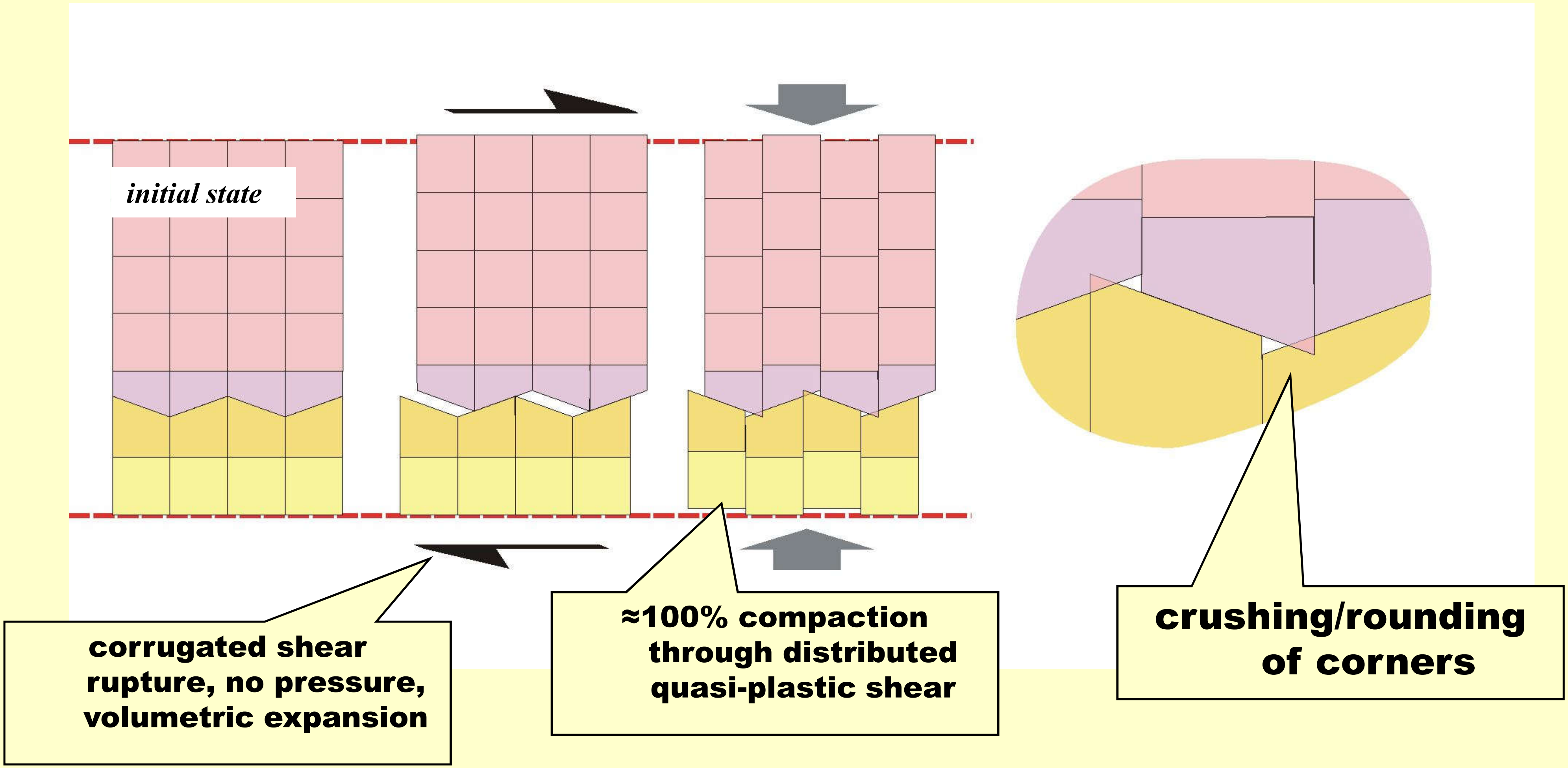

to reduce total sheared area
may operate on a fractal system of subblocks

may operate for larger-scale heterogeneity

Sliding along a corrugated fault: no block rotation, rounded blocks

case 2: excess of material transported to a nearest place of deficit (and vice versa)

"mutual annihilation of material overhang and free space"

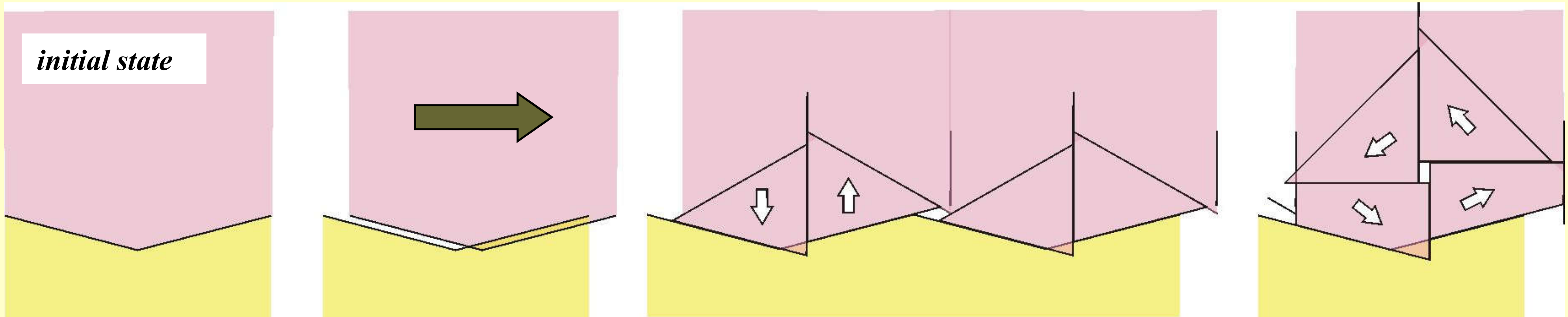

formation of overhang and free space

transfer of the overhang to the free space,

minimum 2 blocks added

transfer of the overhang to the free space,

more blocks

no distributed quasi-plastic outside vicinity of the fault

may operate for smaller-scale heterogeneity

Sliding along a corrugated fault: no block rotation, rounded blocks ; case 2- continued:

formation of "rhomboid"/"lens"/"almond" structure pattern – well known in seismogeology:

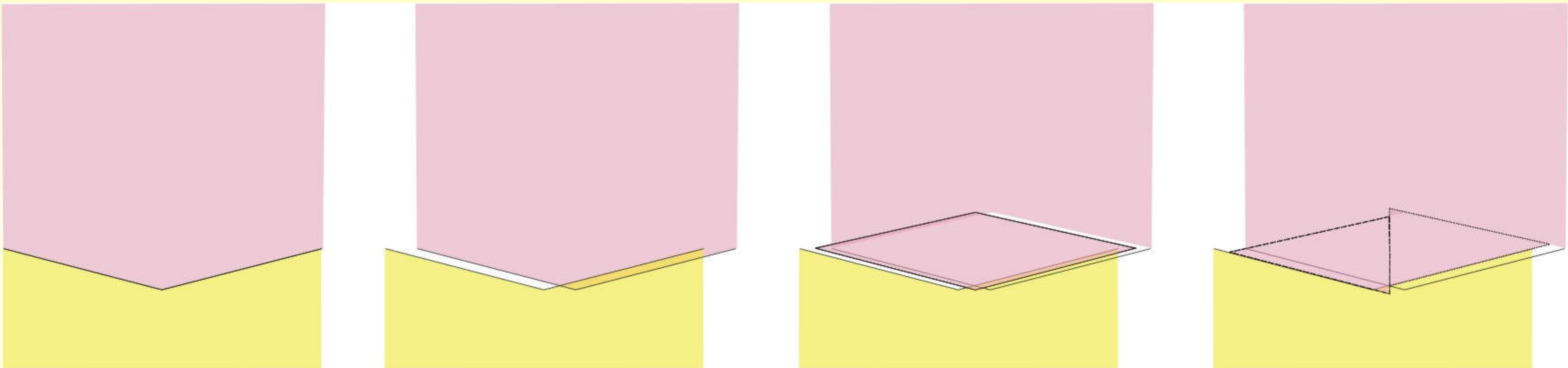

initial state

formation of overhang and free space

formation of a rhomboid - stage 1

free space and overhang conserved

formation of a rhomboid - stage 2

deformation of the rhomboid;

free space and overhang annihilate

rounded blocks case 2:

general situation: no geometric match of fault walls assumed

to eliminate mismatch and free space on a larger scale, a hierarchy of smaller block sizes and motions is needed

simultaneously

excess-deficit annihilation at smaller scales takes place

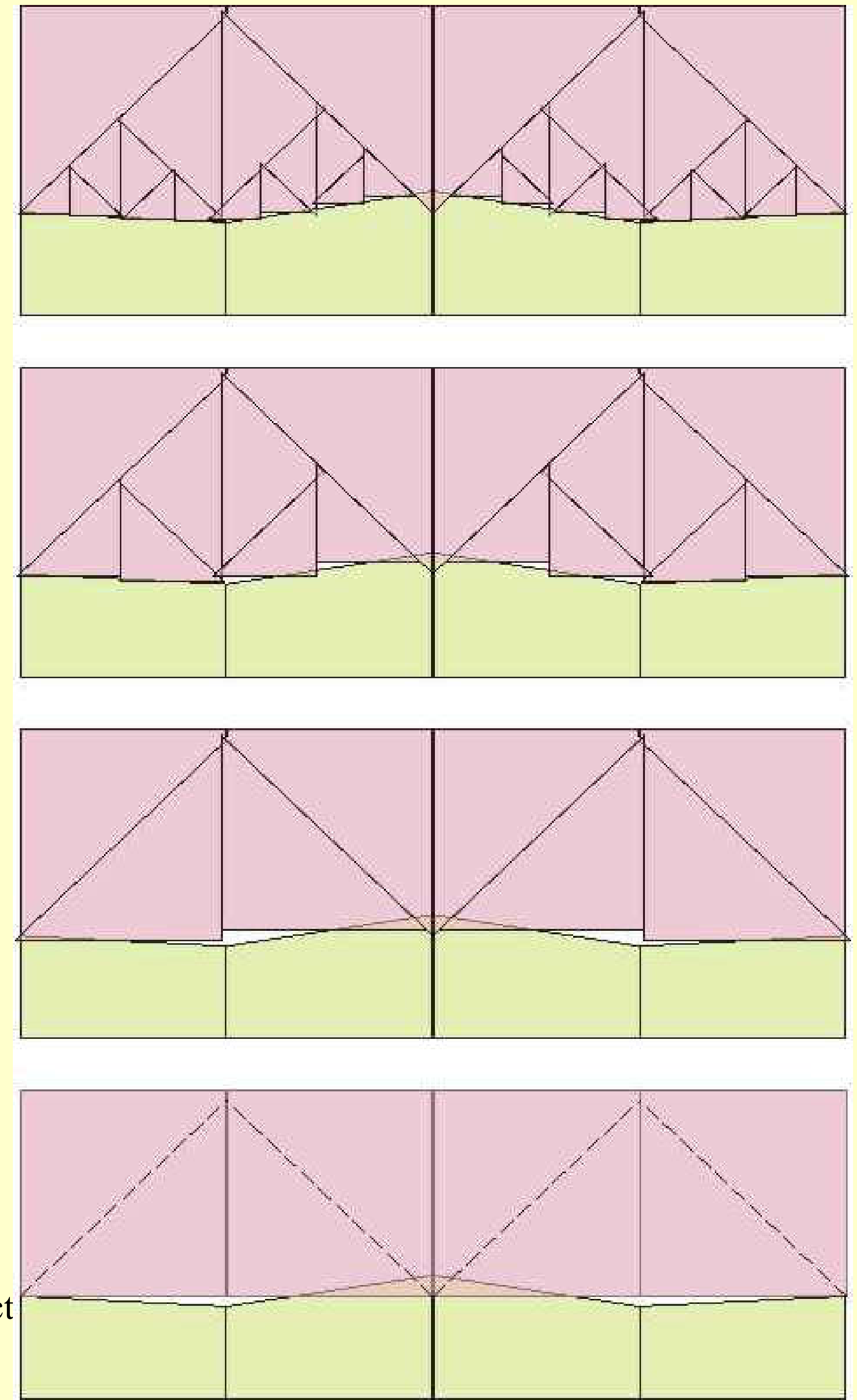

Conclusions on discontinuous fault

1. To explain why neither significant free volume nor unrealistically high overstresses appear around an evolving earthquake fault at long time scales, one can introduce discontinuous medium model with hierarchy of block sizes.
2. This discontinuous medium model can explain fault properties both over short (earthquake) and long (geological evolution) time scales.
3. The assumed system of blocks can mostly eliminate hypothetic obstacles to fault sliding in the form of hills of fault profile. The actual cause for the formation of strength heterogeneity seem to be related to crushing of fresh material at corners of blocks.
4. This heterogeneity forms over multiple scales; this fact explains fractal-like behavior of earthquake rupture

Conclusions

(1) HF radiation bears significant information regarding earthquake fault formation and dynamics

(2) Non-planar, rough, multiscaled fault geometry is a good candidate to simultaneously explain both properties of HF energy generation and of fault dynamics

FIN

Disjointed, fragmented rupture front to explain weak HF directivity:

sharp front and crack tip is possibly a LF-only concept (Gusev 1988)

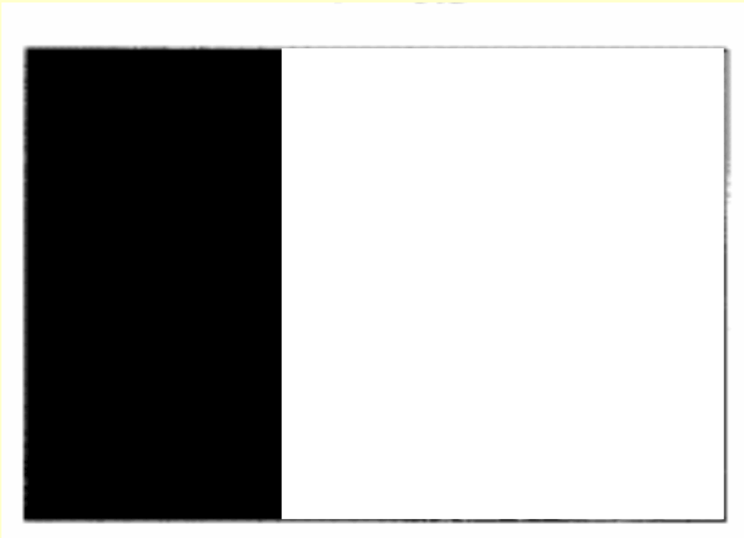

Rupture front / crack tip as ideal object and as modeling instrument at lower frequencies

**Rupture front / crack tip -
more realistic representation,
may be more adequate for broad-band source description**

**To explain very limited HF directivity
One *needs*
incoherent, randomly phased rupture front**

**Illustration from
"Dynamics and Scaling Characteristics of Shear Crack Propagation"
Silberschmidt (2000)**

Examples of coseismic/early postseismic motion along branch/ secondary faults from INSAR images

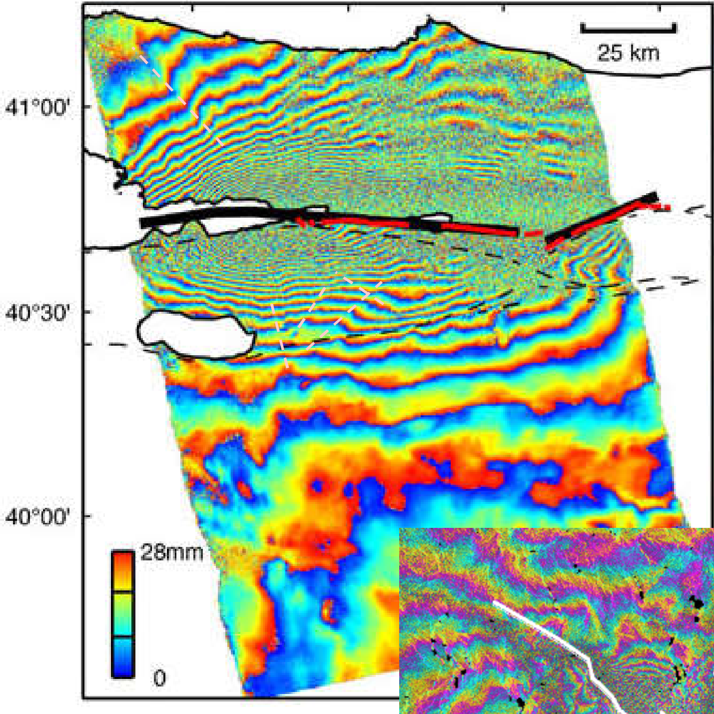

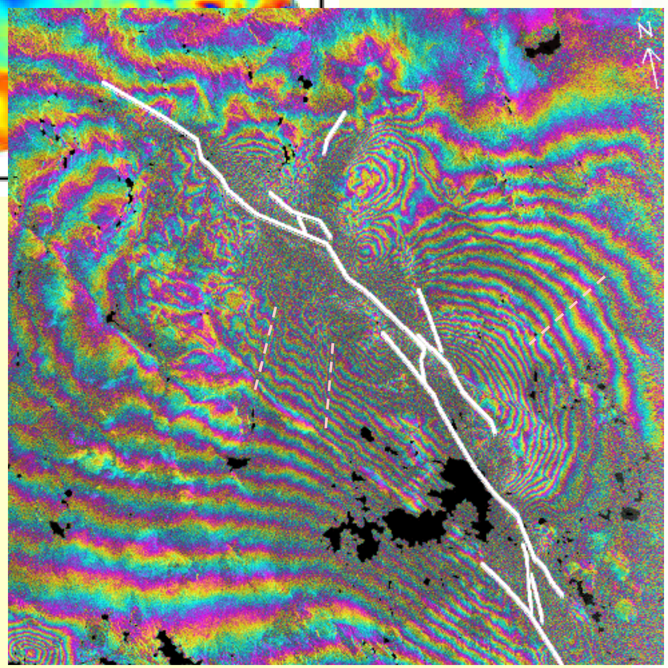

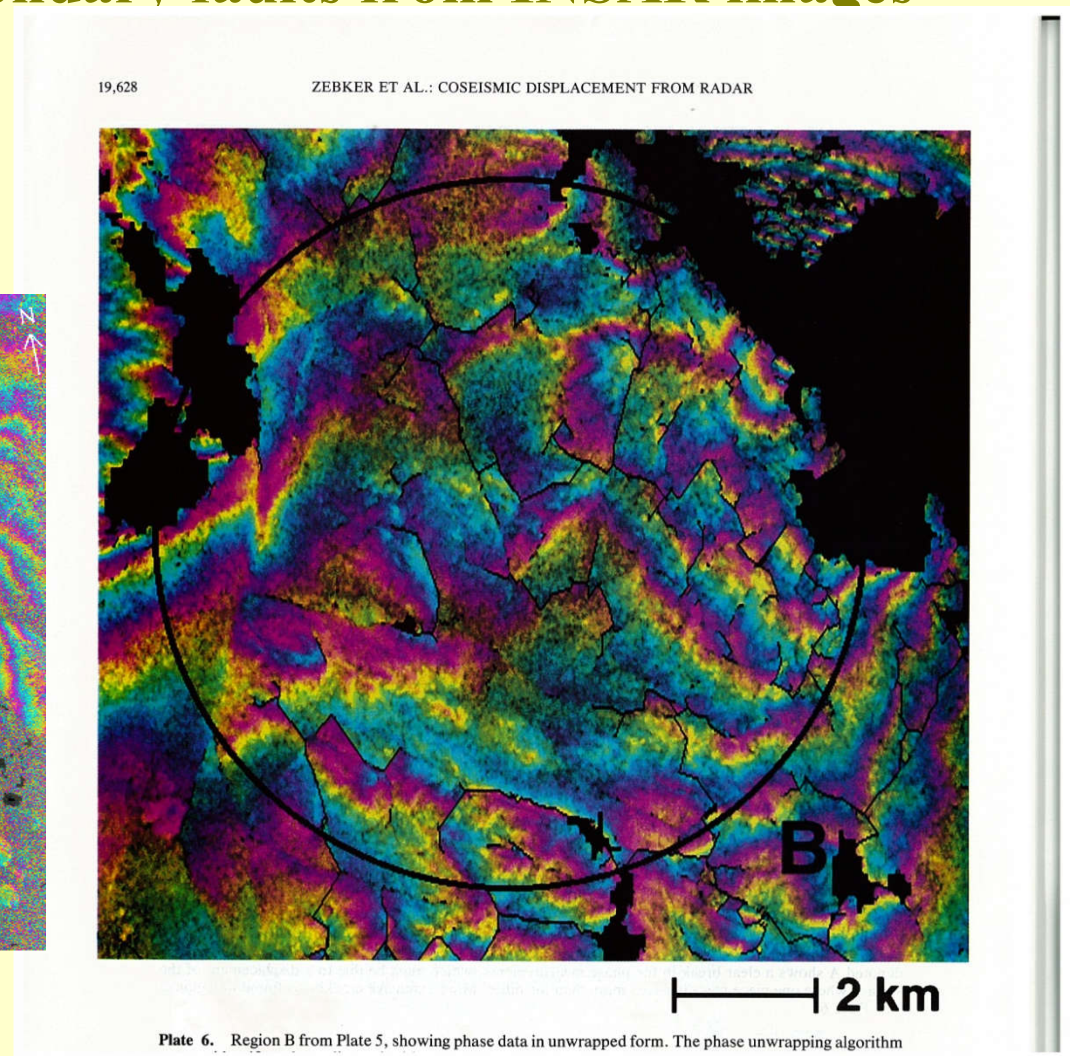

Empirical spectral scaling laws (Halldorsson&Papageorgiou 2005)

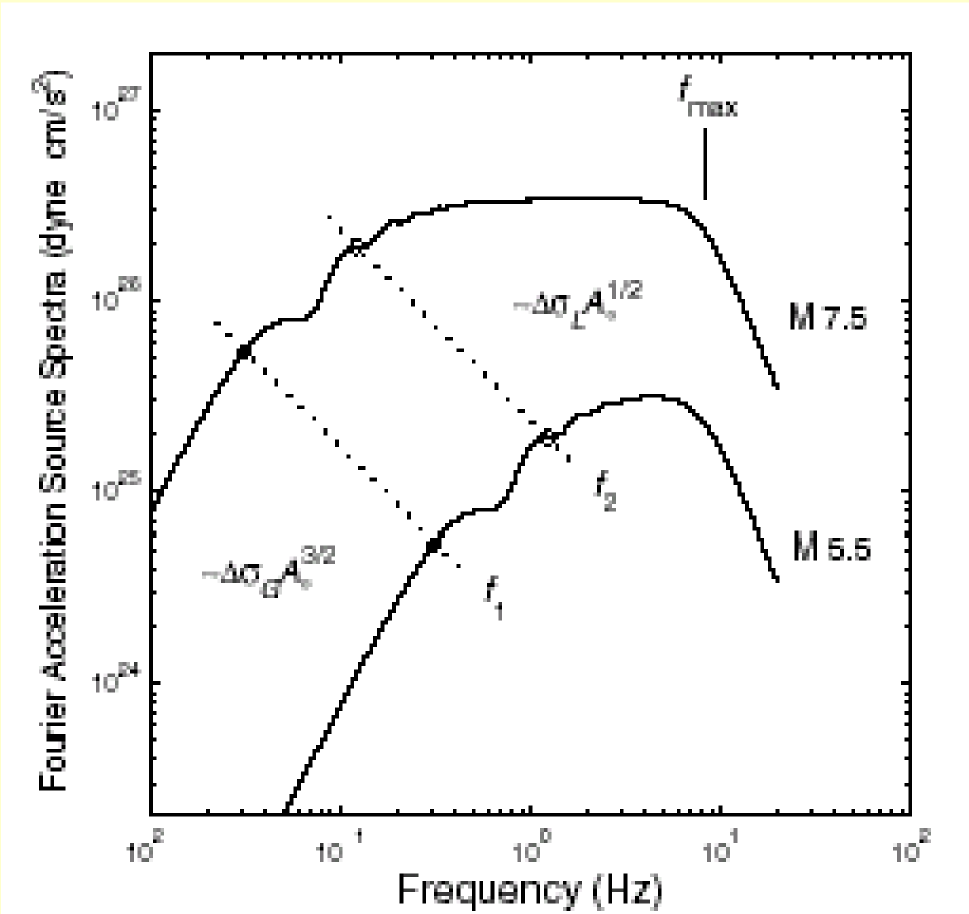

(Halldorsson&Papageorgiou 2005)

f_2 is definitively present

but is scales as f_c

Possible confusion of source-related and medium/path-related effects

•Random-like record: significant contribution from scattering is common

•Spikes: .... path effects suppress spikes

•Directivity: .... scattering reduces directivity

•Spectral shape:...... ϖ^{-2} *behavior*:
magnitude-independent HF energy density, with important exclusion
lack of scaling:
poorly understood, may be related to non-scaling asperity statistics

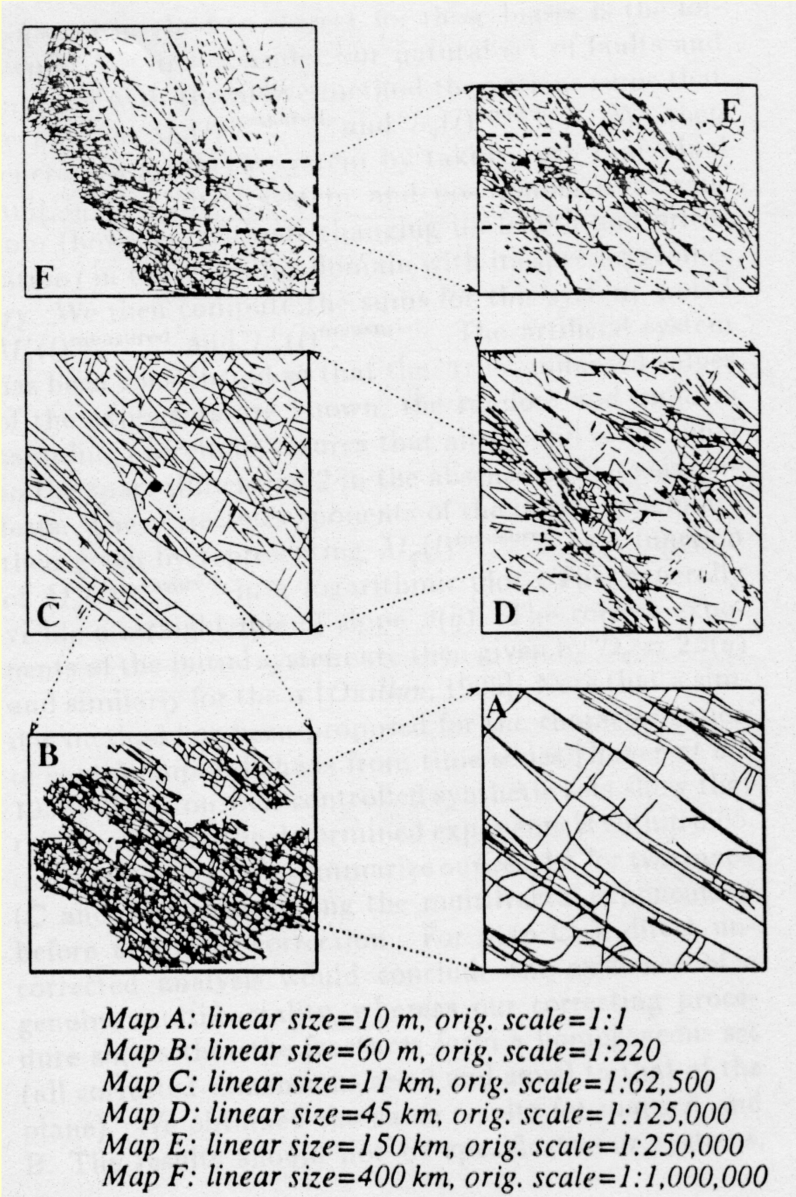

Figure 2. Fracture networks used in this study.

Multiscaled nature of non-planar fault geometry

Significantly deteriorated HF directivity as compared to low-frequency band (2):

$$D = \frac{dx/v_r}{dt} = \left(1 - \frac{v_r}{\beta}\cos\theta\right)^{-1},$$

Example: a_{rms} observed vs. a_{rms} calculated assuming directivity as D^p with various p

(1989 Imperial Valley eq., C.-C. P. Tsai 1997)

negative evidence:

abundant empirical regressions for peak acceleration never included directivity effects

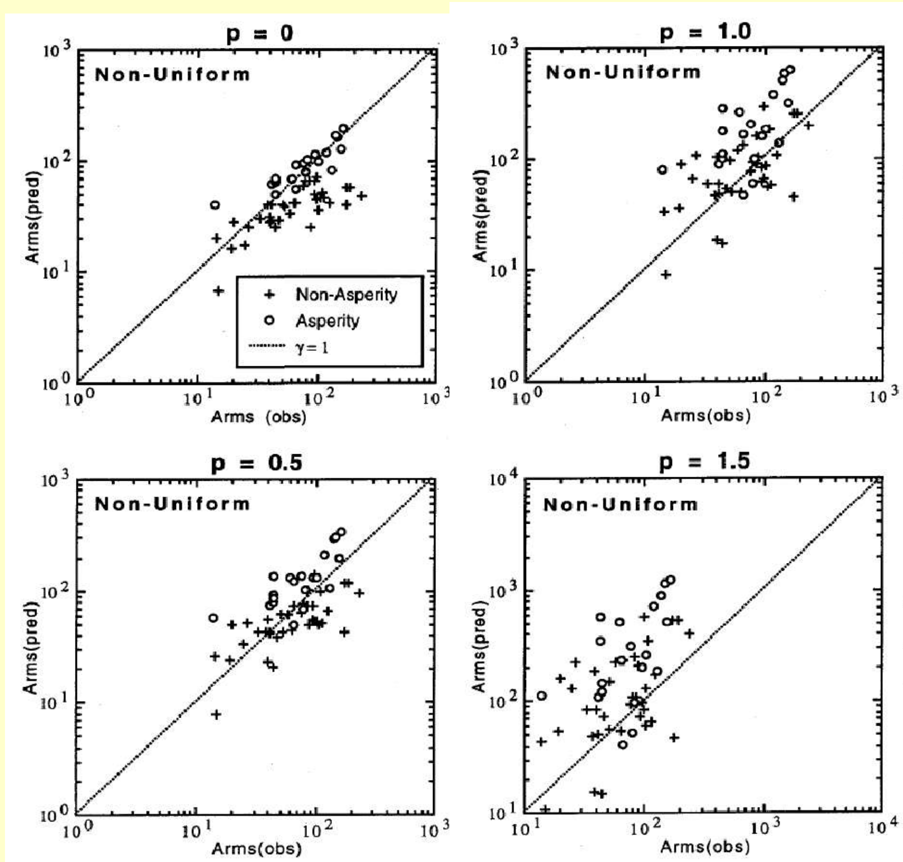

Best fit obtained with *p*=0-0.5

clearly worse fit with *p*=1, 1.5

Explanation (possible) of two acceleration spectral levels [Izutani 1984]

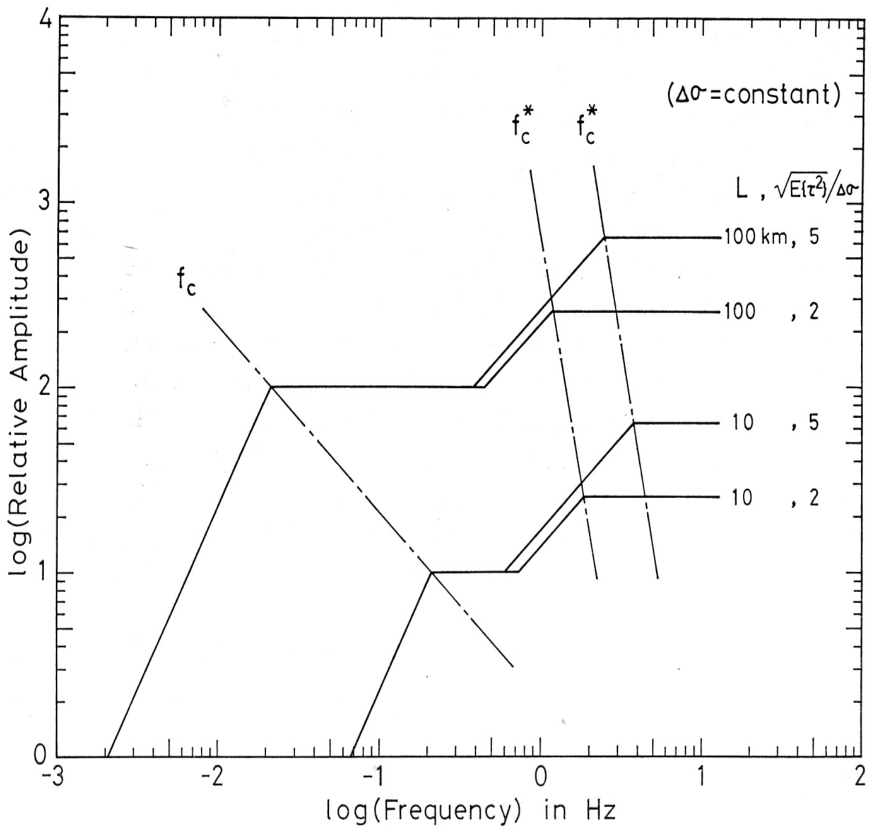

Fig. 6. Acceleration source spectra expected from the present result. The global stress-drop $\Delta\sigma$ is assumed to be constant. f_c and f_c^* are the corner frequency and the second corner frequency, respectively. L is the characteristic length of a fault plane, and $\sqrt{E\{\tau^2\}}/\Delta\sigma$ is the ratio of the rms stress-drop to the global stress-drop.

Stress drop estimate based on **HF acceleration spectrum level** is related to **RMS LOCAL STRESS DROP**

whereas stress drop based on **size-related corner frequency** is defined by **TRUE GLOBAL STRESS DROP**

These two stress drop estimates **need not be proportional to one another**

Relationship between local slip and local HF radiation capability-example

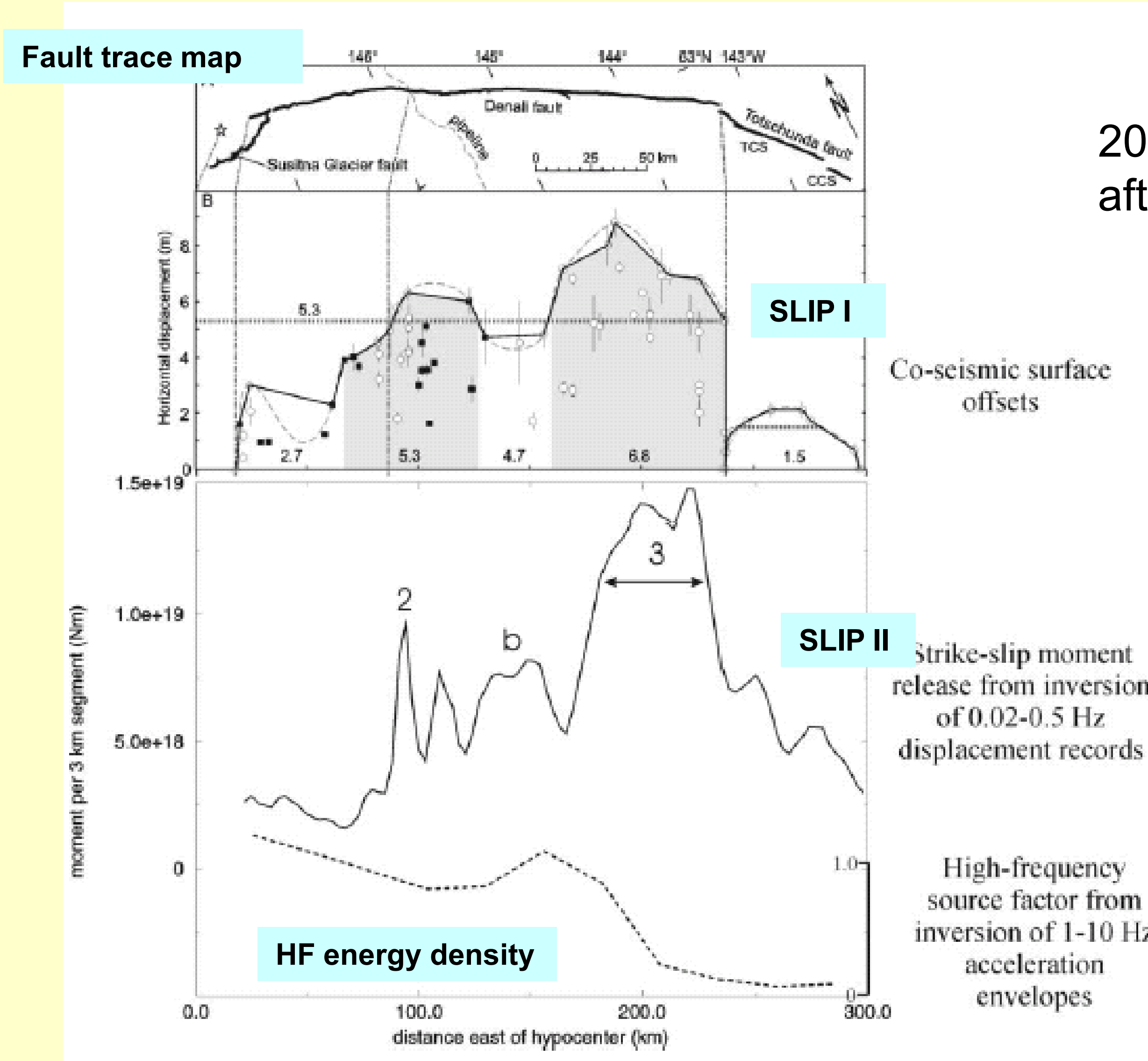

2002, M7.7, Denali, after Frankel 2004

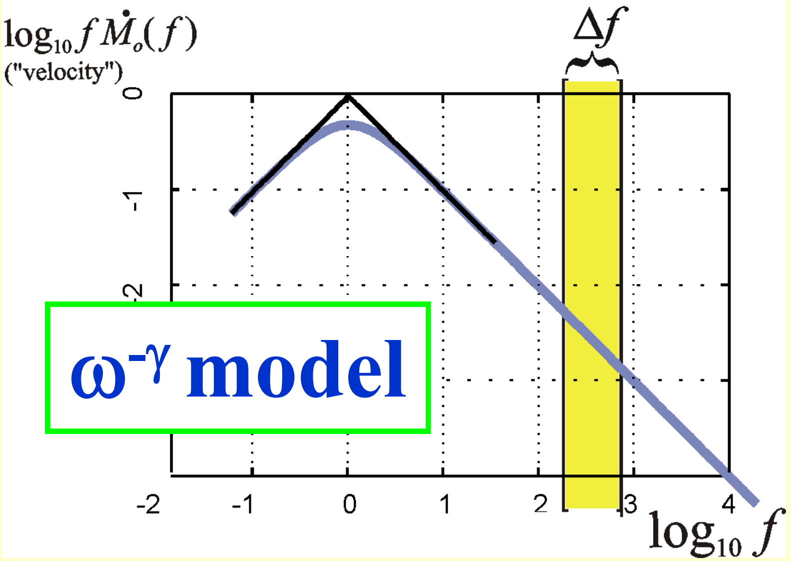

Why ω^{-2} spectral shape?

$$E_s \propto \int_{f_0}^{f_0+\Delta f} \left(\frac{f M_0}{1+(f/f_c)^{\gamma}} \right)^2 df; \quad E_{s,HF} = E_s \Big|_{f_0 >> f_c},$$

$$\left.\frac{\Delta E_{s,HF}}{\Delta f}\right|_{f_0,\Delta f} = W \propto M_0^2 f_c^{2\gamma} \propto M_0^{2-2\gamma/3} \propto S^{3-\gamma}$$

HF energy spectral density

$$\gamma = 3 \quad W \propto M_0^0 \propto \text{const}$$

$$\gamma = 2 \quad W \propto M_0^{2/3} \propto S; \quad \leftarrow dW/dS = \text{const}$$

HF spectral luminosity

$$\gamma = 1.7 \quad W \propto M_0^{0.867} \propto S^{1.3}$$

$$E_{s,tot} \propto M_0 \propto M_0^2 f_c^3 \propto S^{3/2}$$

Spectral energy density: dE/df

Spectral luminosity: $dE/dfdS$

ω^{-2} model predicts
(realistically in zero approximation):
(1) flat spectral shape
(2) scaling of HF spectral level $\sim M_o^{1/3}$

ω^{-2} spectra produce constant HF energy spectral density per unit area (constant *spectral luminosity*)

suggesting HF energy to be produced by the *presence* of rupture front but not by its *amplitude*

Non-Gaussian peaks of accelerograms: 32 records, Δ-30-100 km, M>7,Mexico

original data:

event 1 event 2

GUSEV: NON-GAUSSIAN PEAKS OF MEXICAN ACCELEROGRAMS 20,087

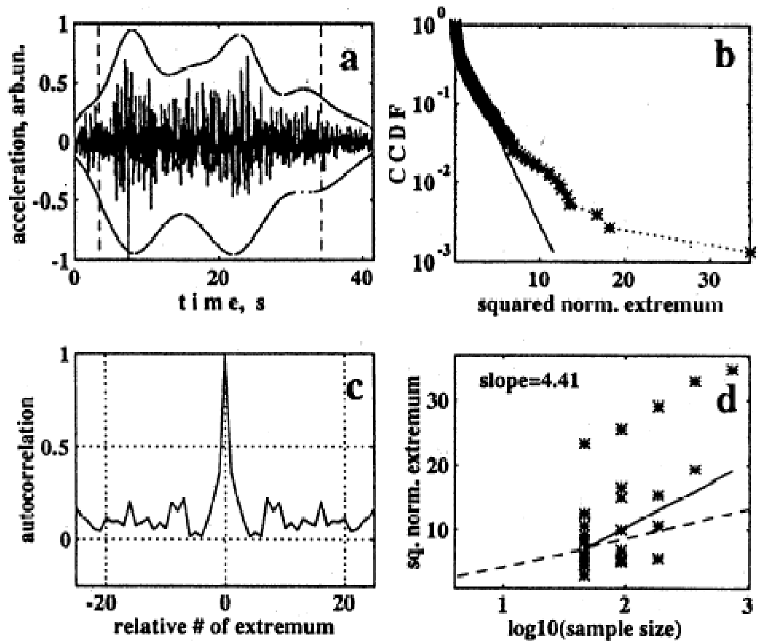

Figure 2. Statistical analysis of the original accelerogram of the September 21, 1985, event at the station UNIO, component N-S. (a) Time history. (b) CCDF of its squared extrema. (c) Autocorrelation of extrema. (d) Squared extremum versus sample size, that is the number of

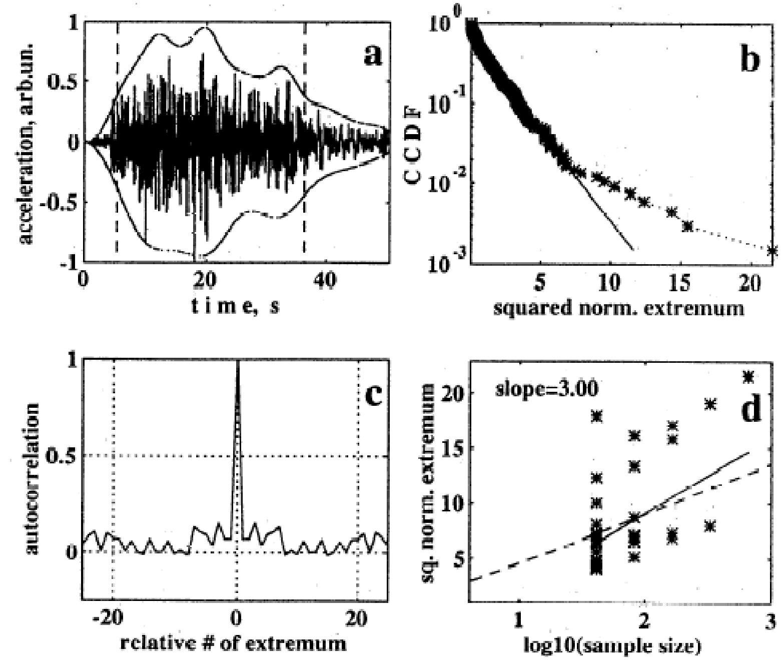

Figure 4. Same as Figure 2, for the September 19, 1985, event at the station CALE, component E-W.

Non-Gaussian peaks of accelerograms in Mexico (2)

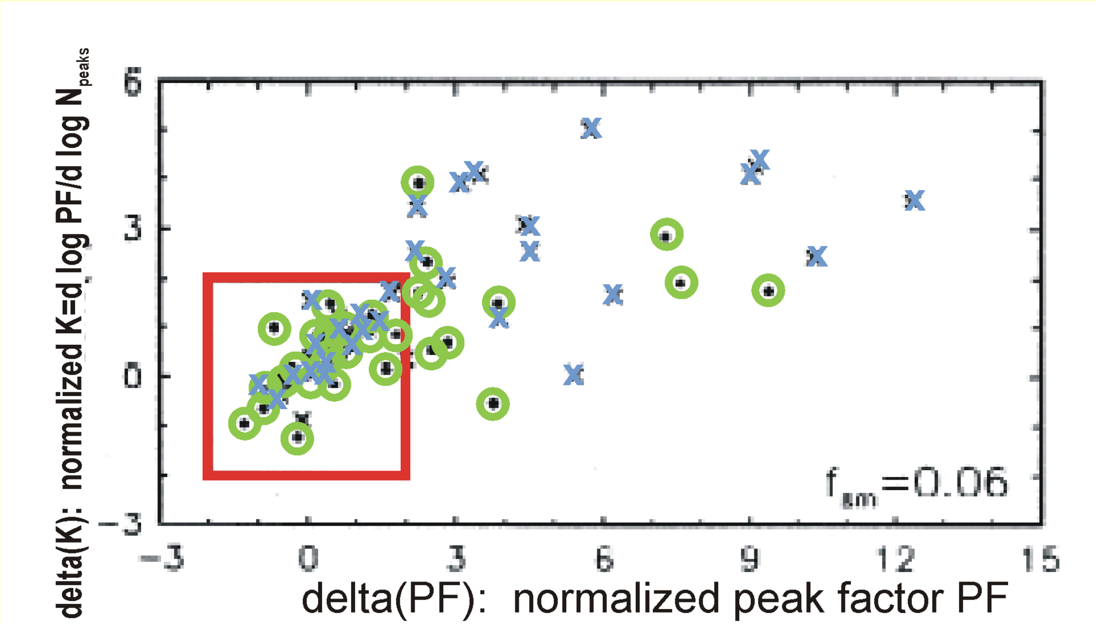

Peak factor:	**$PF=a_{peak}/a_{rms}$**
PF growth rate:	**$K=d\ PF^2 / dlnN_{extrema}$**

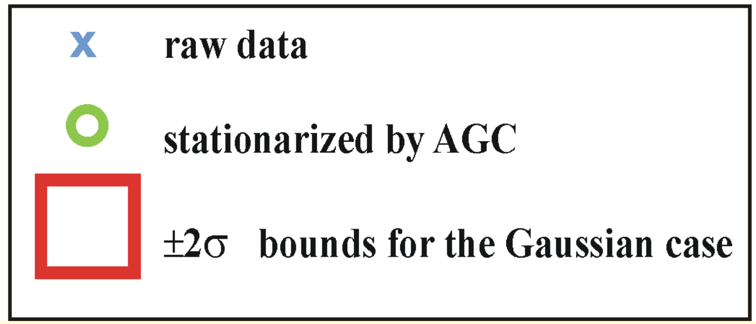

$PF=a_{peak}/a_{rms}$	**delta(PF)=(PF-PF(Gauss))/s(PF)**
$K=d\ PF^2 / dlnN_{extrema}$	**delta(K)=(K-K(Gauss))/s(K)**

From the Peak Factor data,
the estimate for the α parameter in
$pdf(x) \propto x^{-\alpha}$
is about **α = 4.5-5**;
probably overestimation

Probability distributions of final slip: examples from strong motion inversions

[Mendoza and Hartzell (1989)]

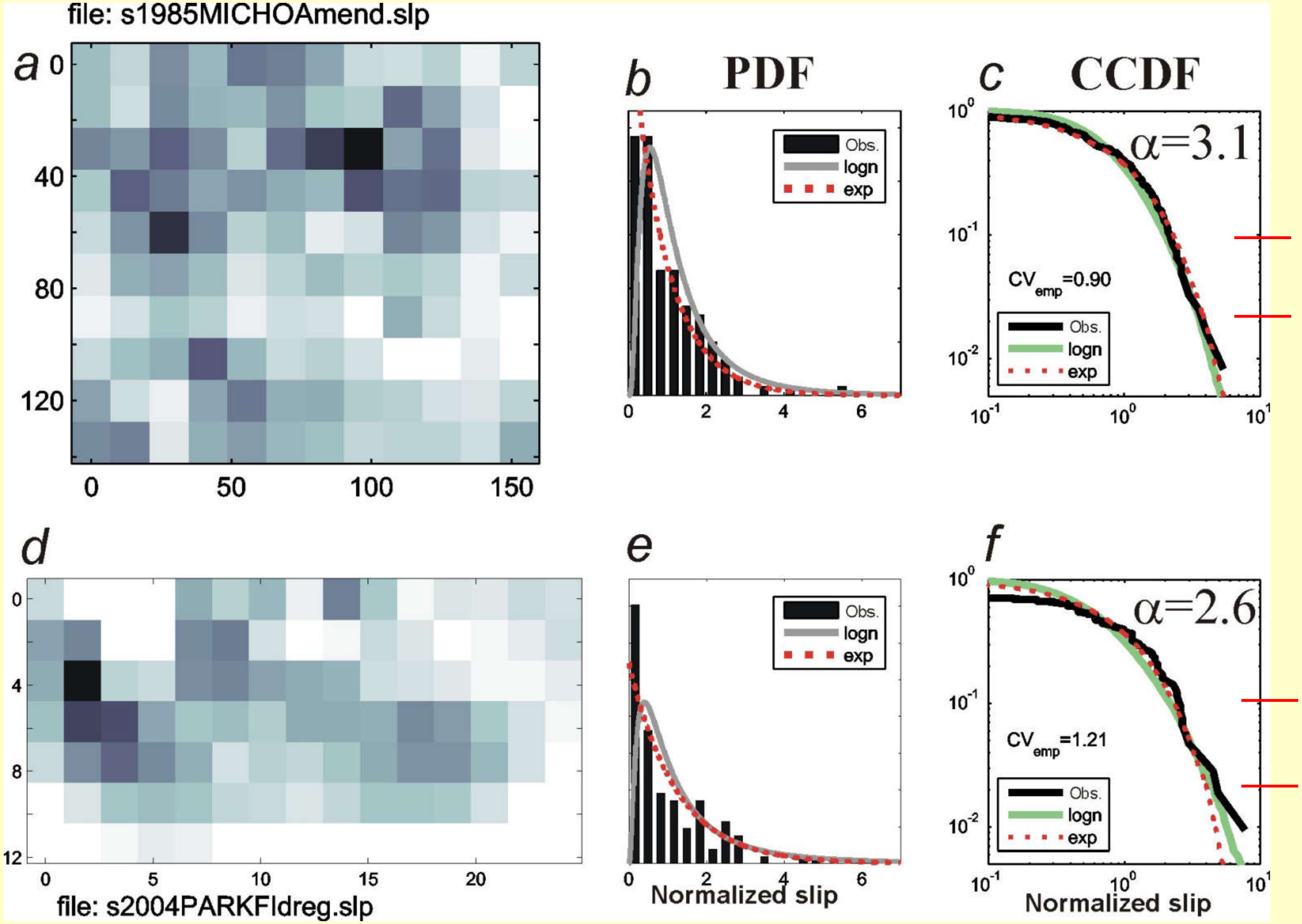

The estimates of α are based on the slope of CCDF between upper quantiles 10% and 2%

[Dreger et al (2004)]

"Source" and body wave (amplitude) Fourier spectra: deterministic vs. "stochastic" viewpoint

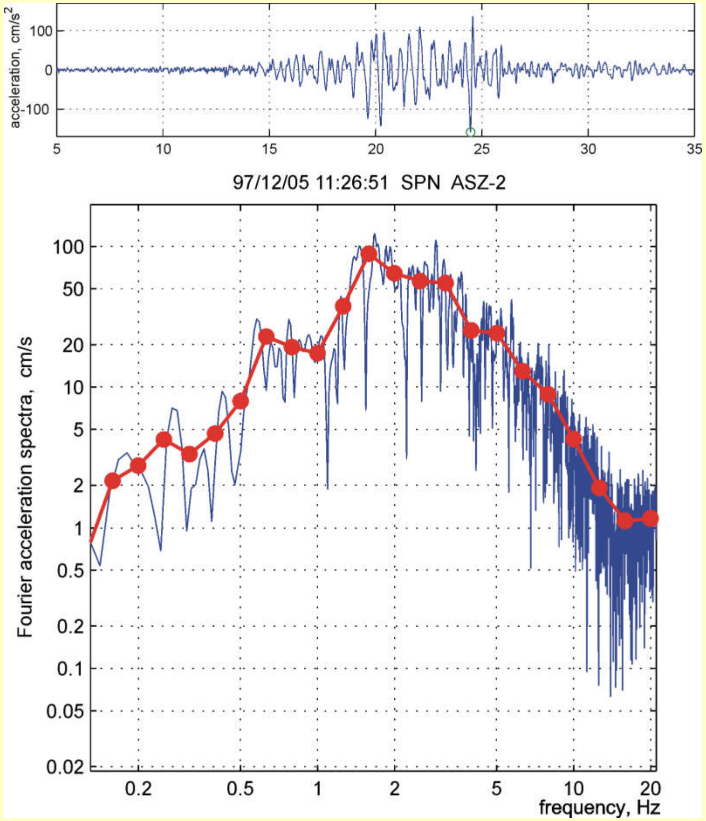

raw FS

smoothed FS

Deterministic view**:**

1. "Raw", unsmoothed Fourier amplitude spectrum: ***the only real object***
2. Smoothed Fourier amplitude spectrum: ***no clear meaning***

"Stochastic" view (***meaningful at HF only***):

1. "Raw", unsmoothed Fourier amplitude spectrum: ***sample function/realization of random process that underlies data***
2. Smoothed Fourier amplitude spectrum: ***empirical estimate for $E^{0.5}(f)$***

   (where $E(f)$ is energy spectral density)

$E^{0.5}(f)$ is a real subject of HF spectral models,
implicitly assumed to be a smooth function of frequency

Empirical/descriptive wideband spectral model [(Gusev 1983 and later work)]

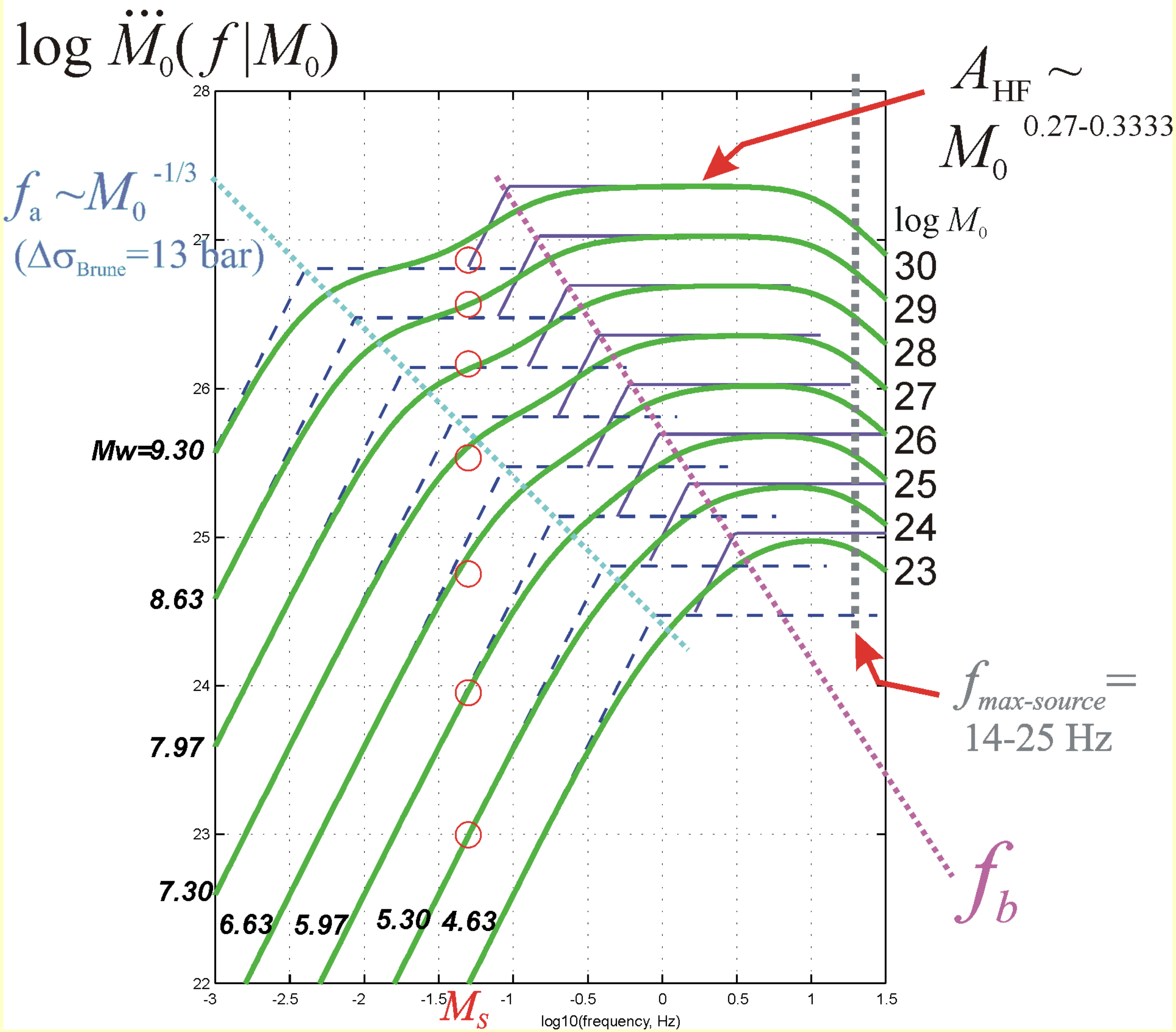

Schematic scaling based on work of Atkinson, Boore, Silva, Papageorgiou, Halldorfson, Dan, Irikura, Morikawa, Fujiwara

Empirical/descriptive wideband spectral model (2) [(Gusev 1983 and later work)]

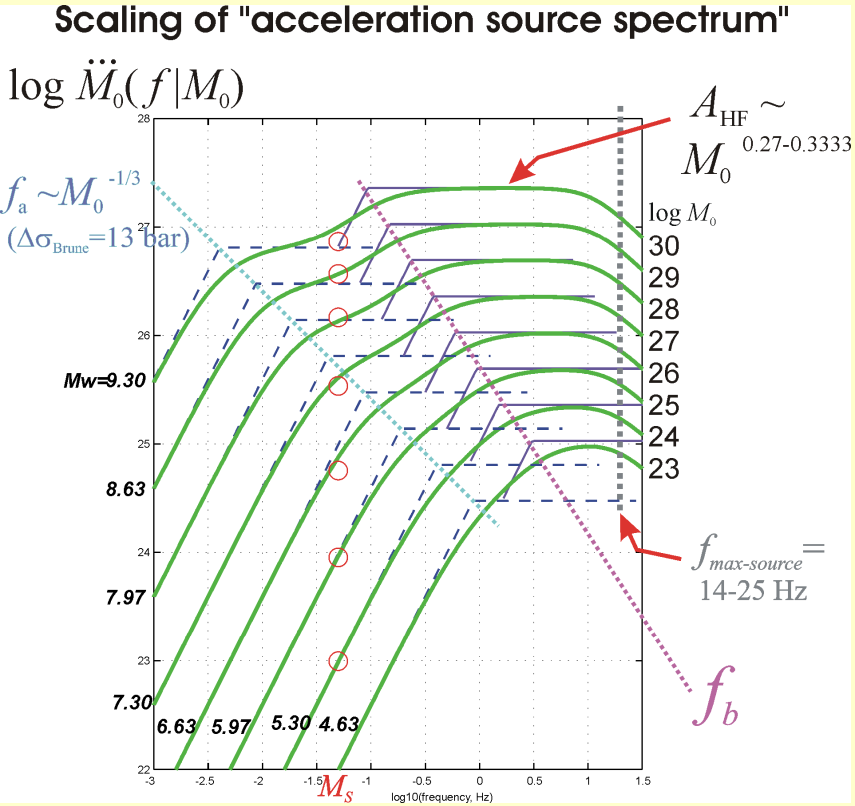

Main features

1. At LF, common scaling ($\boldsymbol{M_o \propto f_a^{-3}}$)
   around common corner frequency $\boldsymbol{f_a}$ (like in ω^{-2} model)

2. Characteristic frequency $f_2 = \boldsymbol{f_b}$ around 0.3- 1 Hz,
   in addition to $f_{corner} = f_a$.
   $\boldsymbol{f_b}$ is ***not proportional*** to $\boldsymbol{f_a}$: no simple similitude,

4. Flat HF [apprx.1-8 Hz] spectral level;
   $\boldsymbol{A_{HF}} \propto M_o^{1/3}$ approx. (like in ω^{-2} model)

5. "Brune stress drops" based on $\boldsymbol{A_{HF}}$
   are 3-6 times above those based on $\{\boldsymbol{f_a}, \boldsymbol{M_0}\}$

6. A source-related HF cutoff frequency, "$\boldsymbol{f_{max\text{-}source}}$",
   is present, in addition to attenuation-related $\boldsymbol{f_{max\text{-}att}}$;
   poorly known

Empirical spectral scaling laws with flat *accelerogram* spectra approximating *source* acceleration shapes

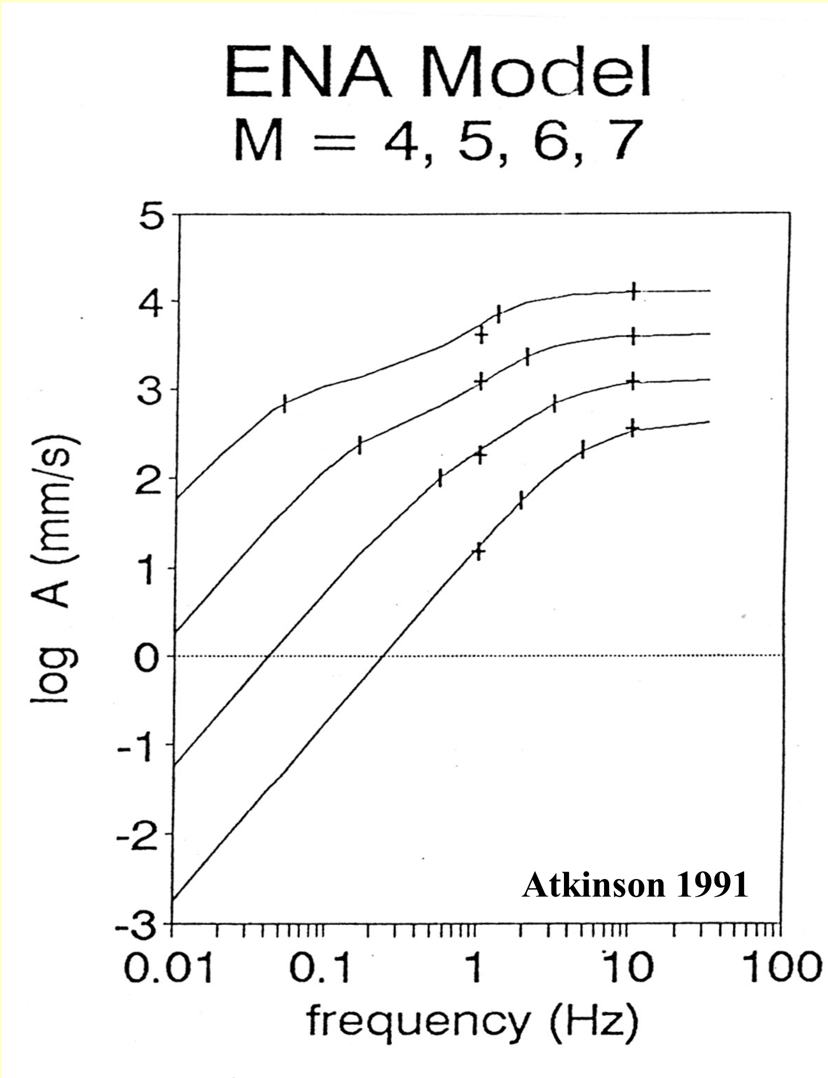

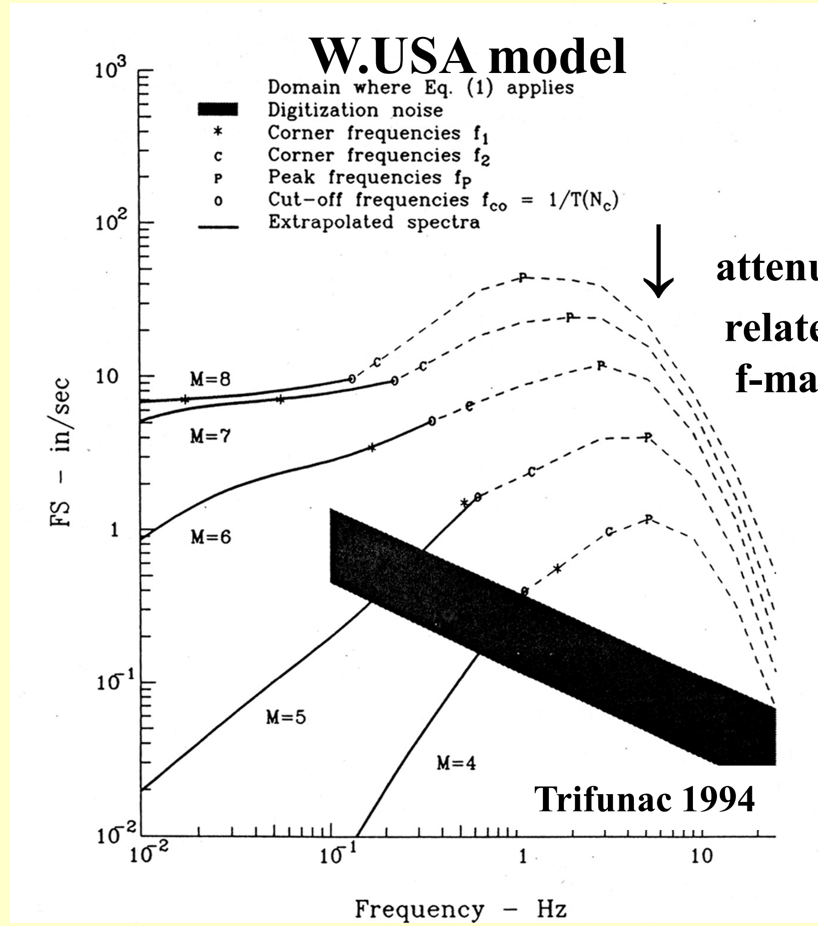

attenuation-related f-max

Illustration of features of observed acceleration spectra

Source-related *f*-max: examples

Low to moderate magnitudes
Instruments in deep boreholes, eliminated attenuation-related f_{max}
Found, typically: source-related f_{max} between 10 and 25 Hz,

Magnitudes 7-8
Pairs of earthquakes recorded at the same station
One of the two events have unusually low source-related $f_{max} \approx 3$ Hz
Attenuation-related f_{max} is present as usual
Can be eliminated by analyzing spectral ratio

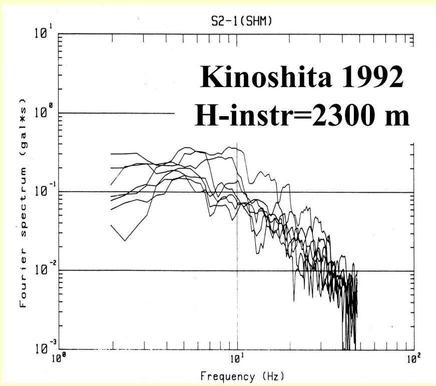

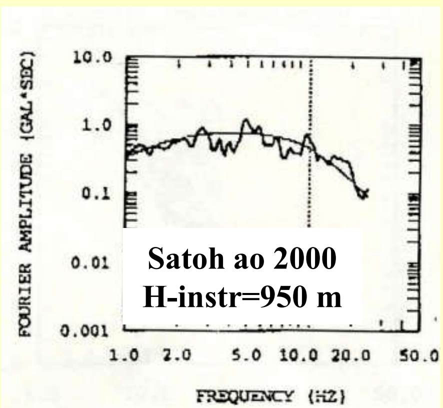

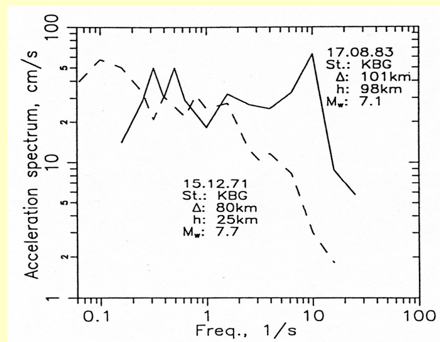

Gusev a.o. 1997

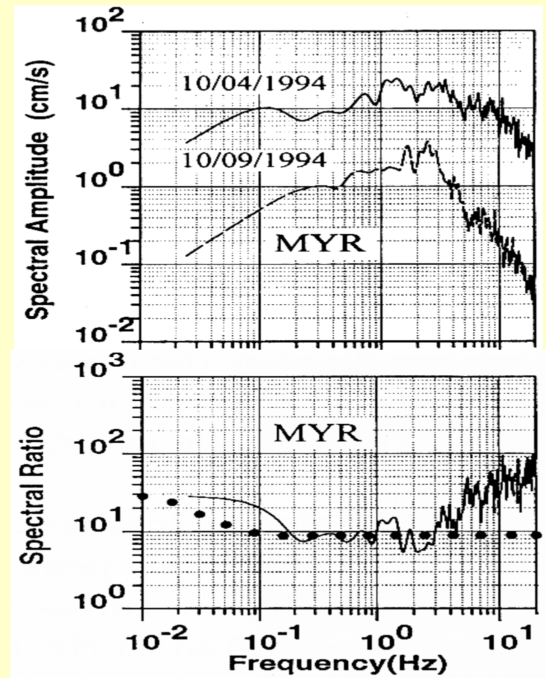

Sasatani 2001

Possible causes for HF properties

•Random-like record: random slip over fault surface $D(x,y)$
random local slip rate history $\mathrm{d}D(t|x,y)/\mathrm{d}t$
random "strength" (definition model-dependent)
??? random rupture tip velocity ???
generally: heterogeneous fault

•Spikes: .... Heavy-tailed stress drop/strength pdf *and/or* arcuate isochrones

•Deteriorated directivity:
.... fragmented, poorly defined rupture tip

•Spectral shape:...... many factors

Part 2.
Models proposed for broad-band source radiation
(descriptive/phenomenological models no dynamics, often poor tectonophysics)

1. Composite sources :
   consisting of subsources of various nature
   (including ones used in engineering-seismology practice)

2. Random function models
   (less developed, no applications)

A.Composite sources

(1) Cracks/patches, overlapping

<<tectonophysically impossible>>

<<works for accelerogram simulation>>

(2) Cracks/patches, non-overlapping/tiling,

a: with non-breakable barrier around each patch

<<tectonophysically improbable>>

<<works for accelerogram simulation>>

b: with barriers that break during current earthquake

<<tectonophysically imaginable,
dynamically doubtful>>

<<not tested for accelerogram simulation>>

(3) Small strong asperities

<<tectonophysically reasonable,
dynamically acceptable>>

<<not tested for accelerogram simulation,
acceptable accelerogram spectra and statistics>>

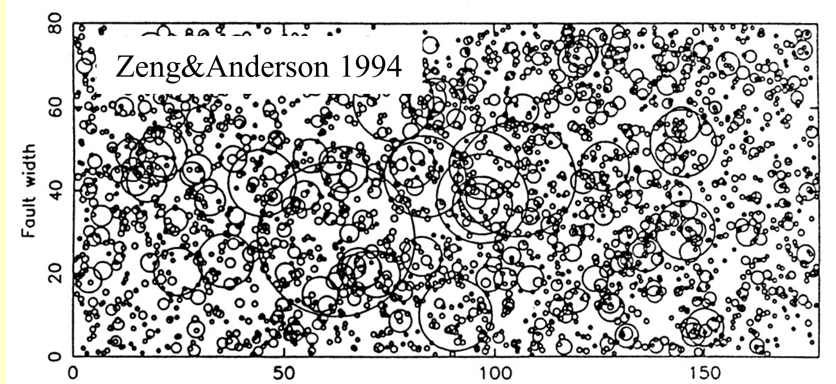

Zeng&Anderson 1994

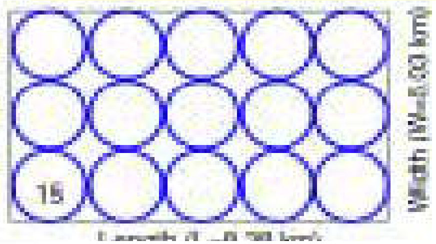

Aki&Papageorgiou 1983

Irikura 1994

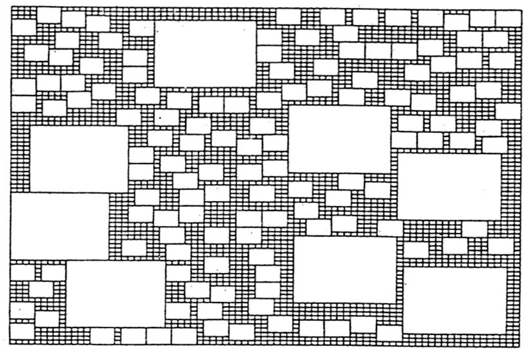

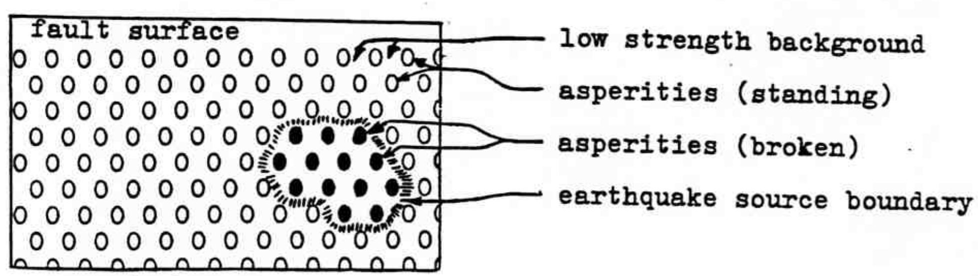

Gusev 1990 following Das& Kostrov 1988

B. Random function models

Random function in space-time specified by
correlation function over x,y,t; or by power spectrum over k_x,k_y,f

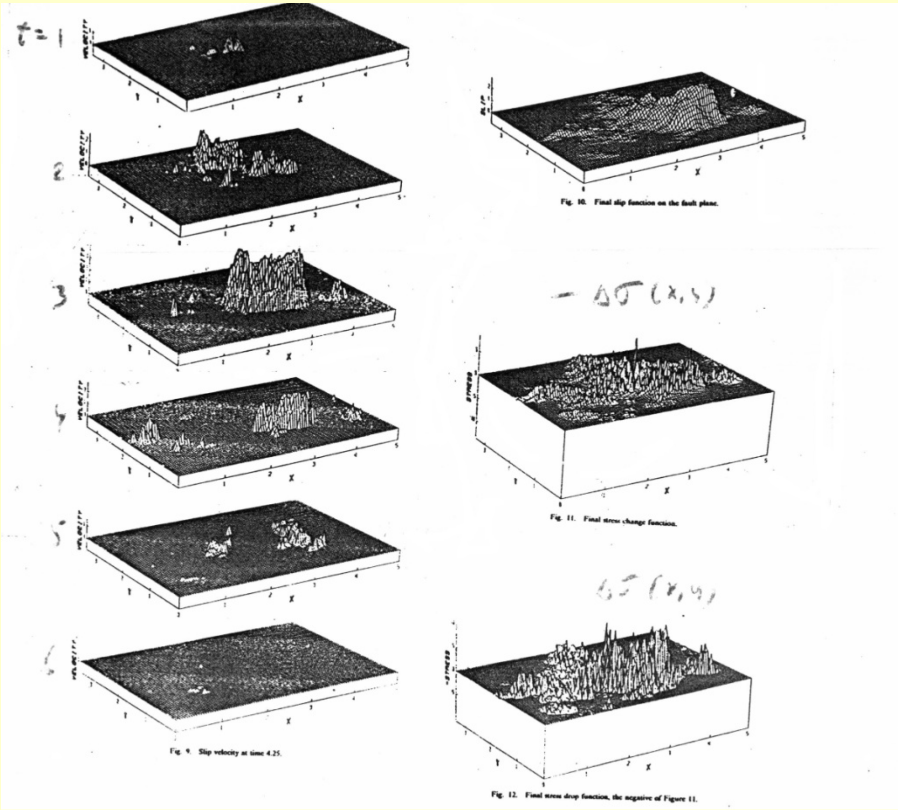

Haskell-Aki 1966-1967:
HF - HK source specified by, effectively,
power-law spectrum in in space-time
<<causal rupture with rupture front
no spikes
partly inconsistent mathematically
numerically not tested, >>

Andrews 1981:
HF - HK source specified by
power-law spectrum in space-time
<<no causality, no rupture front
no spikes
mathematically consistent
numerically tested>>

- **Observed HF radiation from an earthquake fault: properties; relation to fault structure; possible generation mechanisms**
- *A.A. Gusev,*
- *Institute of Volcanology and Seismology, Russian Ac.Sci. and*
- *Kamchatka Branch, Geophysical Service, Russian Ac.Sci., Petropavlovsk-Kamchatsky, Russia*
- **gusev@emsd.ru**
- A. Observed HF radiation from earthquake faults has significant peculiarities, namely
- (1) Random appearance of time functions suggests that ruptures are organized stochastically in a loose sense. Factorization of HF source into well-defined local "history of rise" function and propagating continuous rupture front line may be inadequate.
- (4) HF signals are non-Gaussian, with (moderately) heavy distribution tails, manifested systematically as prominent acceleration spikes. Two causes may be operative in creation such spikes, both quite probable: failure of high-strength fault patches and random rare formation of arc-like coherent features of the rupture front.
- (2) Deteriorated or absent directivity of HF energy suggests irregular geometry of rupture front at high wavenumbers. Locally, rupture velocity may have random magnitude and random orientation. Rupture front may be idealized as a propagating fractal "line", tortuous and, generally, disconnected.
- (3) Fault-controlled Fmax is revealed unequivocally only in rare cases. I believe that this feature, mostly in the range 10-50 Hz, is actually a common one; scarcity of its observations seem be related to technical difficulties. When real, Fmax provides estimates of the upper fractal limit of the above-mentioned rupture front geometry.
- (5) Recently, data have been collected that permit to compare the distribution of HF radiation capability in space-time over the area of a propagation fault, with similar distribution of local slip rate. No good correlation has been revealed.
- (6) Similar descripancy can be seen in spectral domain. Recently, stohastic structure of envelopes of band-filtered HF teleseismic P waves of large earthquakes has been systematically analysed. Clear features of self-similar (fractal) behavior have been revealed, both for teleseismically recorded and for source-radiated signals. This is established for the frequency range from f-corner to 1Hz for teleseismic data, and less reliably from f-corner to 20 Hz for accelerogram data. These facts do not match the behavior of broad-band source spectra where no accurate fractal scaling is observed. (The multiplicity of temporal scales in source formation is a well-established general fact; what is lacking for broad-band signals is self-similarity in a more formal sense. Note that for large earthquakes, the common assumption of the omega-square model typically represents rather crude simplification.)
- The listed properties bear important information regarding fault structure in space-time, and, ideally, are to be emulated by advanced fault models.
- B. One of the main causes of multiple-scaled complexity of ruptures and their radiation may be related to non-flat, random fault geometry, also with multiplicity of scales. It can be shown that relative sliding of monolithic and rough fault walls with realistic multiple-scaled random relief leads to unlimited gaping formation and thus cannot be supported in geological time. To explain why this unlimited gaping is never ovserved, one has to drop that assumption of monolithic behavior of fault walls. They must be assumed discontinuous, consisting of multiple blocks permitting relative motion. This motion may be localized near to the fault, or may extend to the day surface or ductile deep layers. Block shapes may be stable only as a rough approximation; gradual crushing of material must arise around corners of individual blocks. Along the main fault, random normal stress concentrations will be formed. These concentrations lead to intermittent shear strength distribution (barriers and asperities) that eventually explain many properties of HF radiation.